PLOS Climate

Tracking and forecasting community responses to climate perturbations in the California Current Ecosystem

--Manuscript Draft--

Manuscript Number:	PCLM-D-21-00040
Article Type:	Research Article
Full Title:	Tracking and forecasting community responses to climate perturbations in the California Current Ecosystem
Short Title:	Tracking and forecasting community state
Corresponding Author:	Mary Hunsicker NOAA Fisheries Newport, OR UNITED STATES
Order of Authors:	Mary E. Hunsicker
	Eric J. Ward
	Michael A. Litzow
	Sean C. Anderson
	Chris J. Harvey
	John C. Field
	Jin Gao
	Michael G. Jacox
	Sharon Melin
	Andrew R. Thompson
	Pete Warzybok
Keywords:	Climate variability; climate change; marine heat wave; extreme events; regime shift; ecosystem state; novel state; forecasting; multivariate time series analysis; Dynamic Factor Analysis; north Pacific Ocean; California Current; seabirds; marine mammals; fish
Abstract:	Ocean ecosystems are vulnerable to climate-driven perturbations, which are increasing in frequency and can have profound effects on marine social-ecological systems. Thus, there is an urgency to develop tools that can detect the response of ecosystem components to these perturbations as early as possible. We used Bayesian Dynamic Factor Analysis (DFA) to develop a community state indicator for the California Current Ecosystem (CCE) to track the system's response to climate perturbations, and to forecast future changes in community state. Our key objectives were to (1) summarize environmental and biological variability in the southern and central regions of the CCE during a recent and unprecedented marine heatwave in the northeast Pacific Ocean (2014–2016) and compare these patterns to past variability, (2) examine whether there is evidence of a shift in the community to a new state in response to the heatwave, (3) identify relationships between community variability and climate variables; and (4) test our ability to create one-year ahead forecasts of individual species responses and the broader community response based on ocean conditions. Our analysis detected a community response to the marine heatwave, although it did not exceed normal variability over the past six decades (1951-2017), and we did not find evidence of a shift to a new community state. We found that nitrate flux through the base of the mixed layer exhibited the strongest relationship with species and community-level responses. Furthermore, we demonstrated skill in creating forecasts of species responses and community state based on estimates of nitrate flux. Our indicator and forecasts of community state show promise as tools for informing ecosystem-based and climate-ready fisheries management in the CCE. Our modeling framework is also widely applicable to other ecosystems where scientists and managers are faced with the challenge of managing and protecting living marine resources in a rapidly changing

	climate.
Opposed Reviewers:	
Additional Information:	
Question	**Response**
Financial Disclosure Enter a financial disclosure statement that describes the sources of funding for the work included in this submission and the role the funder(s) played. This includes grants and any commercial funding of the work or authors. This statement will be typeset if the manuscript is accepted for publication. *Please review the submission guidelines and the instructions link below for detailed requirements and guidance.*	Funding for this project came from NOAA's Fisheries and the Environment (FATE) program (project 16-01) and NOAA's California Current Integrated Ecosystem Assessment program.
Competing Interests On behalf of all authors, disclose any competing interests that could be perceived to bias this work. This statement will be typeset if the manuscript is accepted for publication. *Please review the instructions link below and PLOS Climate's competing interests policy to determine what information must be disclosed at submission.*	The authors do not have any competing interests (financial or non-financial) with respect to the work presented in this research article.
Data Availability Before publication, Authors are required to make fully available and without restriction all data underlying their findings. Please see our PLOS Data Policy page for detailed information on this policy.	All time series collected through the CalCOFI and RREAS surveys are available through ERDDAP data server. We encourage readers to contact Dr. Andrew Thompson (CalCOFI) and Dr. John Field (RREAS), who have expert knowledge about the surveys and data, if they are interested in accessing the data. The seabird and sea lion time series are available through the California Current Integrated Ecosystem Assessment (CCIEA) web dashboard, CCIEA annual reports, and the CalCOFI State of the California Current Reports. We encourage readers to contact Dr. Pete Warzybok (seabird data) and Dr. Sharon Melin (sea lion data) about these data sets if they are interested in accessing them.

A **Data Availability Statement**, detailing where the data can be accessed, is required at first submission. Insert your Data Availability Statement in the box below. Please see the data reporting section of our submission guidelines for instructions on what you need to include in your Data Availability Statement. This statement will be typeset if the manuscript is accepted for publication. *PLOS allows rare exemptions to address legal and ethical concerns. If you have legal or ethical restrictions, please use the box below to detail these in full sentences for the Journal team to consider.*	

September 24, 2021

Dear Dr. Archer,

Climate perturbations are having strong impacts on ocean ecosystems that in turn affect social and economic components of human communities. These effects may be exacerbated when changes in ocean conditions are more extreme, such as during marine heatwaves. The increasing attention on these extreme events and their impacts has invigorated a push for tools that can track and detect as early as possible the response of marine communities to climate-driven perturbations. In the attached manuscript, entitled "Tracking and forecasting community responses to climate perturbations in the California Current Ecosystem", we build on a novel set of statistical tools that we previously developed to generate indicators of community state and to identify potential shifts to a novel state. Specifically, we expand a Bayesian implementation of a multivariate time series analysis, Dynamic Factor Analysis, to test community responses to climate variables within the modeling framework and to develop near-term forecasts of future community states. We apply this analysis to the California Current Ecosystem (CCE) to document the community response to climate perturbations over the past six decades, including a recent marine heatwave, and forecast the community response one year ahead. While the focus of our study is the CCE, the approach applied here is widely applicable to the myriad marine ecosystems worldwide that are vulnerable to a rapidly changing climate.

Our analysis produced multiple informative and valuable findings. For example, we detected a community response to the 2014-2016 northeast Pacific marine heatwave; however, it did not exceed normal variability within the study timeframe or result in a shift to a novel community state. We also identified relationships between community state and multiple climate variables, with nitrate flux having the strongest correspondence with individual species time series and the shared trend in community variability. Moreover, we demonstrated skill in creating simultaneous one-year lead time forecasts of species responses and community state.

We are submitting our paper as a research article to *PLOS Climate* as we believe it will be of broad interest to the readership of *PLOS Climate* and the broader *PLOS* community. Our approach for developing a community state indicator has the potential to support ecosystem-based and climate-ready management in multiple ways. Garnering knowledge of community state and the potential for large shifts in ecosystem structure in response to intense and novel climate perturbations can help inform better, more rapid management decisions for mitigating ecological and socioeconomic impacts.

The research and results presented here are novel from any past work I, or my colleagues, have done. This work has not yet been published, has been approved for publication by all authors, and has only been submitted to *PLOS Climate* for consideration. Thank you for considering our manuscript for publication. We look forward to hearing from you.

Sincerely, on behalf of all co-authors,

Mary E. Hunsicker

Short Title: Tracking and forecasting community state

Tracking and forecasting community responses to climate perturbations in the California Current Ecosystem

Mary E. Hunsicker[1,†,*], Eric J. Ward[2,†], Michael A. Litzow[3], Sean C. Anderson[4], Chris J. Harvey[2], John C. Field[5], Jin Gao[6], Michael G. Jacox[7], Sharon Melin[8], Andrew R. Thompson[9], Pete Warzybok[10]

[1]Fish Ecology Division, Northwest Fisheries Science Center, National Marine Fisheries Service, National Oceanic and Atmospheric Administration, 2032 SE OSU Drive, Newport, OR 97365 US
[2]Conservation Biology Division, Northwest Fisheries Science Center, National Marine Fisheries Service, National Oceanic and Atmospheric Administration, Seattle, WA 98112 USA
[3]Alaska Fisheries Science Center, National Marine Fisheries Service, National Oceanic and Atmospheric Administration, Kodiak, AK 99615 USA
[4]Pacific Biological Station, Fisheries and Oceans Canada, Nanaimo, BC V9T 6N7 Canada
[5]Fisheries Ecology Division, Southwest Fisheries Science Center, National Marine Fisheries Service, National Oceanic and Atmospheric Administration, Santa Cruz, CA USA
[6]Centre for Fisheries Ecosystems Research, Memorial University of Newfoundland, St. John's, NL A1C 5R3 Canada
[7]Environmental Research Division, Southwest Fisheries Science Center, National Marine Fisheries Service, National Oceanic and Atmospheric Administration, Monterey, CA 93940 USA / Physical Sciences Laboratory, National Oceanic and Atmospheric Administration, Boulder, CO 80305 USA.
[8]Marine Mammal Laboratory, Alaska Fisheries Science Center, National Marine Fisheries Service, National Oceanic and Atmospheric Administration, Seattle, WA 98115 US
[9]Southwest Fisheries Science Center, National Marine Fisheries Service, National Oceanic and Atmospheric Administration, La Jolla, CA USA
[10]Point Blue Conservation Science, Petaluma, CA USA

*Corresponding author
Email: mary.hunsicker@noaa.gov

† These authors contributed equally to this work

Abstract

Ocean ecosystems are vulnerable to climate-driven perturbations, which are increasing in frequency and can have profound effects on marine social-ecological systems. Thus, there is an urgency to develop tools that can detect the response of ecosystem components to these perturbations as early as possible. We used Bayesian Dynamic Factor Analysis (DFA) to develop a community state indicator for the California Current Ecosystem (CCE) to track the system's response to climate perturbations, and to forecast future changes in community state. Our key objectives were to (1) summarize environmental and biological variability in the southern and central regions of the CCE during a recent and unprecedented marine heatwave in the northeast Pacific Ocean (2014–2016) and compare these patterns to past variability, (2) examine whether there is evidence of a shift in the community to a new state in response to the heatwave, (3) identify relationships between community variability and climate variables; and (4) test our ability to create one-year ahead forecasts of individual species responses and the broader community response based on ocean conditions. Our analysis detected a community response to the marine heatwave, although it did not exceed normal variability over the past six decades (1951-2017), and we did not find evidence of a shift to a new community state. We found that nitrate flux through the base of the mixed layer exhibited the strongest relationship with species and community-level responses. Furthermore, we demonstrated skill in creating forecasts of species responses and community state based on estimates of nitrate flux. Our indicator and forecasts of community state show promise as tools for informing ecosystem-based and climate-ready fisheries management in the CCE. Our modeling framework is also widely applicable to other ecosystems where scientists and managers are faced with the challenge of managing and protecting living marine resources in a rapidly changing climate.

Introduction

Climate perturbations can have strong impacts on ocean ecosystems that in turn affect social and economic components of human communities. These effects may be exacerbated when changes in ocean conditions are more extreme, such as during marine heatwaves. The increasing attention on these extreme events and their impacts (e.g., Hobday et al. 2018, Sen Gupta et al. 2020) has invigorated a push for tools that can track and detect as early as possible the response of marine communities to climate-driven perturbations. Early detection, and moreover, near-term forecasts of community shifts could help scientists, managers, and stakeholders better prepare for and respond to the potential consequences of such shifts.

Climate-driven shifts in community structure tend to involve rapid change across multiple populations that result in switches between contrasting community assemblages that may then persist for decades. A growing number of studies have documented community reorganizations in response to climate drivers (e.g., Beaugrand et al. 2008, 2015, Möllman and Diekmann 2012, Wernberg et al. 2016, Peabody et al. 2018). One of the best-known examples is the widespread northeast Pacific community reorganization that followed the 1976/1977 shift in the Pacific Decadal Oscillation (Benson and Trites 2002; Hare and Mantua 2000). The abrupt change from a cool to warm ocean regime had dramatic implications on ecosystem functioning and living marine resources (LMRs) throughout the region (Mantua et al. 1997, Anderson and Piatt 1999; Litzow and Ciannelli 2007, Peabody et al. 2018). Since then, northeast Pacific marine ecosystems have experienced several interannual or decadal perturbations that do not appear to have resulted in community-wide shifts of similar magnitude. However, between 2014 and 2016 these ecosystems experienced a marine heatwave that involved the warmest sea surface temperature (SST) and heat content anomalies that had ever been observed over large areas of

82 the North Pacific (Bond et al. 2015; Walsh et al. 2018). It was one of the most extreme
83 heatwaves globally in its combined magnitude, spatial scale, and duration (Hobday et al. 2018,
84 Sen Gupta et al. 2020), and the intense, persistent warming has been attributed to a combination
85 of natural and anthropogenic forcing (Jacox et al. 2018a; Laufkötter et al. 2020).
86 Several studies have documented myriad biological responses to this event. For example,
87 within the California Current Ecosystem (CCE), there were mass strandings of marine mammals
88 (Cavole et al. 2016), increased whale entanglements due to shifting prey sources (Santora et al.
89 2020), mass mortality events for marine seabirds (Cavole et al. 2016, Jones et al. 2018, Piatt et
90 al. 2020), a record-breaking domoic acid outbreak (McCabe et al. 2016), shifts in pelagic
91 macronekton and micronekton communities and species richness (Santora et al. 2017, Brodeur et
92 al. 2019, Nielsen et al. 2020), irruptions of previously rare fishes and invertebrates throughout
93 the California Current (Sakuma et al. 2016, Morgan et al. 2019, Sanford et al. 2019, Walker et al.
94 2020), and extraordinarily high recruitment of rockfishes (genus *Sebastes*; Schroeder et al. 2018,
95 Field et al. 2021) and northern anchovy (*Engraulis mordax*; Thompson et al. 2019). Yet, to date,
96 there have been few quantitative studies of how the marine heatwave impacted the broader CCE
97 community at multiple trophic levels, and therefore the importance of this extreme event for
98 community-wide patterns of variability, and the persistence of the community response, remains
99 largely unknown.
100 Indicators of community or ecosystem state are valuable tools for tracking climate-related
101 changes in ecosystem functioning and evaluating those changes within the context of past
102 climate perturbations (Harvey et al. 2020). Moreover, combining long-term monitoring surveys
103 and data with modeling frameworks that summarize information across taxa and life stages that
104 respond quickly to climate perturbations could provide early detection of an ecosystem shifting

105 into a novel state. Early detection of such shifts would benefit ecosystem-based and climate-
106 ready fisheries management strategies aimed at mitigating possible deleterious ecological and
107 socio-economic outcomes. There is also a pressing need for forecasts of future ecosystem states
108 to support forward-looking management of LMRs (Hobday et al. 2016, Tommasi et al. 2017,
109 Jacox et al. 2020), including assessments of risk. As climate models and forecasts of ocean
110 conditions continue to improve, the time is ripe for developing and testing methods that could
111 provide near-term forecasts of community state in relation to ocean conditions.
112 A challenge in summarizing ecosystem responses to perturbations is that time series used
113 to characterize the ecosystem often involve tens to hundreds of variables (species or climate
114 indices); there is often some degree of asynchrony among time series, and further, each is
115 corrupted by the presence of observation errors. Disentangling these sources of error and
116 separating the signal from the noise is statistically challenging. Traditionally, tools such as
117 Principal Components Analysis (PCA) or nonmetric multidimensional scaling have often been
118 used for identifying leading patterns of variability in multivariate datasets (e.g., Koslow et al.
119 2002, 2013); however, these approaches are ill-suited to the analysis of time series data that are
120 autocorrelated or non-stationary (Planque and Arneberg 2018). An alternative approach,
121 Dynamic Factor Analysis (DFA), is better suited for identifying shared trends that can be used as
122 a community state indicator. DFA is specifically designed for time series ordination, and avoids
123 many of the problems associated with other multi-variate approaches (Zuur et al. 2003). When
124 applied to a collection of multivariate time series, inference in DFA models focuses on
125 estimating a smaller number of temporal patterns ('trends') that best capture the variation
126 observed. The observed data are then treated as a mixture of these trends (Ward et al. 2019).
127 Ward et al. (2019) recently developed a Bayesian implementation of DFA that models shared

trends, detects "black swan" events (rare and difficult to predict events; Anderson et al. 2017), and estimates the probability of switches among contrasting system states. In the first application of this new method, Litzow et al. (2020a) examined shared trends of climate and biology time series in the Gulf of Alaska. Their study did not detect evidence for wholesale community reorganization during the recent northeast Pacific marine heatwave; however, their findings indicated potential for new patterns of ecosystem functioning with continued warming of ocean temperatures.

Here we build on this set of novel statistical tools to develop a model of the CCE state that can both track and forecast ecosystem changes in response to climate perturbations. Specifically, we expand the Bayesian implementation of DFA to test the community response to environmental variables within the modeling framework and to develop near-term forecasts of future community states. Using climate and biological data from the central and southern regions of the CCE, our goals were to: (1) summarize environmental and biological variability during 2014–2016 and compare these patterns to past variability; (2) assess the probability of observed departures from previous climate patterns and of switches to new states in community variability during the heatwave; (3) identify relationships, if any, between community variability and climate variables; and (4) test our ability to create one-year ahead simultaneous forecasts of species responses and the community state based on environmental information. While the focus of our study is the CCE, the approach applied here is widely applicable to the myriad marine ecosystems worldwide that are vulnerable to a rapidly changing climate.

Methods

Data

In our analysis, we used oceanographic time series from the southern (n=6) and central (n=6) regions of the CCE, derived from a data assimilative configuration of the Regional Ocean Modeling System (ROMS) with 0.1˚ (~10 km) horizontal resolution and 42 terrain-following vertical levels (Neveu et al. 2016; oceanmodeling.ucsc.edu). From the ROMS output, we generated monthly time series covering 1980-2018 for a suite of variables including sea surface temperature (SST), sea surface height (SSH), isothermal layer depth (ILD), Brunt-Väisälä frequency (BV), a coastal upwelling transport index (CUTI), and a biologically effective upwelling transport index (BEUTI). The ILD is similar to mixed layer depth and defines the depth where temperature deviates by 0.5˚C from the surface value. BV is a measure of water column stratification, averaged over the upper 200 m of the water column. CUTI and BEUTI are upwelling indices that quantify vertical transport and nitrate flux through the base of the mixed layer, respectively (Jacox et al. 2018b). The data were annually averaged (July-June) from the coast to 100 km offshore, with the exception of CUTI and BEUTI, which capture coastal upwelling within 75 km of shore. In the alongshore direction, we calculated averages for two regions with a division at Point Conception, California, separating the southern portion of the CCE (31–34.5˚N) from the central region (34.5-40.5˚N, Fig. 1). The annual averages were taken from July to June to capture the influence of the El Niño–Southern Oscillation (ENSO), which peaks in winter and is the dominant mode of interannual variability influencing the California Current. We developed models using ROMS output rather than empirical measurements because they provide full spatial and temporal coverage of surface and subsurface conditions, incorporate available observations, and will enable the use of ROMS forecasts to then forecast biological changes in the CCE. More details on the oceanographic time series can be found in S1 Table and S1 Figure.

Figure 1. Sampling locations of California Current Ecosystem biology included in the study analyses. Abundance data for pelagic juvenile groundfishes and invertebrates are collected on the Rockfish Recruitment and Ecosystem Assessment Survey (RREAS). Ichthyoplankton data are collected on the California Cooperative Oceanic Fisheries Investigations (CalCOFI) survey. Seabird reproductive success and California sea lion (*Zalophus californianus*) pup time series are collected on Southeast Farallon Island and San Miguel Island, respectively. See S1 Table and S1 Figure for detailed information on the individual time series.

The biology time series included in our analysis were selected based on three criteria: first, the measured variables would be expected to show rapid (0- to 1-year lag) responses to climate variability; second, the time series could be updated with no more than one year lag for processing time to increase the speed at which biological responses to perturbation could be detected; and third, the time series were at least 15 years long. The biology time series that met these criteria (n=38) included ichthyoplankton, pelagic young-of-the-year (juvenile fish), squid, and krill abundance; seabird productivity; and California sea lion pup body condition metrics (Fig. 1, S1 Table). These 38 time series were collected from four disparate ocean surveys, and span between 22 and 68 years. Datasets collected from surveys that included spatial attributes (e.g., ichthyoplankton and pelagic juvenile fish surveys) were first standardized using Generalized Additive Models to create a univariate time series for each species. While these datasets generally include spatial random sampling, the index standardization accounts for uneven distributions of effort (in space or time). Details on the standardization of individual datasets are included in S1 Appendix. In addition, the biology data were normalized with log

197 transformations where appropriate (all zeros were changed to NAs). For example, if the time
198 series data were assumed to be lognormally distributed (e.g., weight/count data) or the
199 coefficient of variation was > 1, the data were log transformed. All of the time series from an
200 individual dataset (survey) were treated the same, i.e., logged or not. More details on the biology
201 time series used in this study and the associated data sources and log transformations are
202 summarized in S1 Table and S1 Figure.
203
204 *Modeling*
205 We describe the methods in detail below, but in summary our work flow was to (1) apply
206 Bayesian DFA to climate and biology datasets separately and use model selection tools to
207 identify the best supported model and number of shared trends, (2) apply 'black swan' and
208 regime detection methods to detect extreme events and alternating community states,
209 respectively, (3) identify whether the CCE community state was strongly correlated with the
210 climate time series (compare performance of the biology models with/without environmental
211 covariates), and (4) evaluate our skill at making predictions of community state and individual
212 species variables.
213
214 *Dynamic Factor Analysis*
215 We used a Bayesian version of Dynamic Factor Analysis (DFA, Zuur et al. 2003, Ward et
216 al. 2019) using the software Stan and R (R Core Team 2018) as implemented in the 'bayesdfa'
217 package (Ward et al. 2020). DFA is a multivariate statistical tool somewhat analogous to
218 Principal Components Analyses, but for time-series data (Holmes et al. 2018, https://cran.r-
219 project.org/web/packages/MARSS/vignettes/UserGuide.pdf). For a collection of time series, the

number of estimated 'trends' is specified *a priori*, and DFA estimates these latent trends as independent random walks. In mathematical form, this is expressed as

$$\boldsymbol{x_t} = \boldsymbol{x_{t-1}} + \boldsymbol{w_{t-1}},$$

where $\boldsymbol{x_t}$ represents the value of latent (unobserved) trends at time *t*, and the process error deviations $\boldsymbol{w_{t-1}}$ are generally assumed to be white noise having arisen from a multivariate normal distribution (with an identity covariance matrix for identifiability). The latent trends are mapped to the observed data through an estimated loadings matrix $\mathbf{Z}$ and residual error $\boldsymbol{e}_t$,

$$\boldsymbol{y}_t = \mathbf{Z}\boldsymbol{x}_t + \boldsymbol{b} \cdot \boldsymbol{d}_t + \boldsymbol{e}_t,$$

where $\boldsymbol{y}_t$ is the vector of observed states at time *t*, and the residual error terms $\boldsymbol{e}_t$ are assumed to be drawn from a univariate or multivariate normal distribution. Though the covariance matrix of $\boldsymbol{w_t}$ is generally fixed (Zuur et al. 2003), the covariance matrix of $\boldsymbol{e}_t$ can be structured; variances may be shared or not across time series, and off diagonal elements may be estimated. The parameter vector $\mathbf{b}$ represents optional estimated coefficients relating covariates $\boldsymbol{d}_t$ to the observed response. In the context of our DFA modeling, we included climate variables as $\boldsymbol{d}_t$ in models where the biological observations were used as the response $\boldsymbol{y}_t$.

Because we implemented the DFA model in a Bayesian setting, we were able to extend this model to include additional features. First, to include extreme events, we relaxed the assumption about process errors $\boldsymbol{w_t}$ being drawn from a normal distribution and used a multivariate Student-t distribution instead (Anderson and Ward 2019). We also modified the process equation to consider an optional vector of AR(1) coefficients $\boldsymbol{\phi}$ on the latent trends. $\boldsymbol{x_t} = \boldsymbol{\phi x_{t-1}} + \boldsymbol{w_{t-1}}$ (Ward et al. 2019). A final modification of the conventional DFA model is that for some models, process variances can be estimated rather than fixed at 1 (maximum likelihood approaches generally use this constraint for identifiability). As implemented in Stan

(Stan Development Team 2016, Hoffman and Gelman 2014, Carpenter et al. 2017), we conducted estimation with three chains, with a warm-up of 2000 samples, followed by 2000 iterations. We used the split-chain potential scale reduction factor (Gelman and Rubin 1992, Gelman et al. 2013) to assess convergence (Rhat < 1.05). Code to replicate these analyses is deployed as an R package on CRAN ('bayesdfa', Ward et al. 2020) and our public Github repository, https://github.com/fate-ewi/bayesdfa.

We ran the DFA on climate datasets (1981–2017) and biological datasets (1951–2017) across the southern and central regions of the California Current combined. Running the analysis at this spatial scale allowed us to capture the broader community response to climate perturbations, compared to running models on each multivariate dataset independently (e.g., time series from a single survey). There are a number of ways to evaluate predictive accuracy of these models. Leave-One-Out Cross-Validation (LOO-CV), for example holds each observation out in turn and predictions are made from the remaining data. As our focus was on the temporal nature of the data and forecasting component, we implemented a variant of k-fold cross validation and treated individual years as unique 'folds'. Because our objectives involved evaluating these models for future predictions, we implemented the Leave-Future-Out Cross Validation Information Criterion (LFO-CV, Bürkner et al. 2020). We used this approach to identify data support for (1) the number of latent DFA trends (n = 1-3), (2) first-order autoregressive AR(1) coefficients on the trends ($\boldsymbol{\phi}$ estimated with a Normal(0,1) prior), (3) Student-t deviations (i.e., evidence of extreme events, using a prior on the MVT degrees of freedom parameter, ν, of $\nu \sim \text{Gamma}(2, 0.1)$), and (4) a fixed versus estimated trend variance (using a prior on the standard deviation, σ_w, of $\sigma_w \sim \text{Normal}(0,1)$).

In addition, we used LFO-CV to identify the most appropriate error structure for the climate dataset—specifically whether the times series had equal (shared) or unequal (unique) observation errors. For the biology models, we assumed the observation errors were unique by dataset, and our estimates of survey variance supported this assumption.

For each model formulation, we applied the LFO-CV method by first fitting the model to all years of data prior to year *T* (i.e., training data) and then using the fitted model to predict the trend value in year *T* (i.e., test data). We repeated this process for 10 years, starting with 2017 as year *T* and working back to 2008, and then calculated the expected log predictive density (ELPD) across those time steps. The climate and biology models with the highest ELPD were deemed the best supported models. The LFO-CV is a preferred method for evaluating future predictive performance of Bayesian models because it properly accounts for time series structure, and unlike other Bayesian cross-validation methods, does not produce overly optimistic estimates (Bürkner et al. 2020).

Detection of extreme events and regime shifts

After identifying the best-supported DFA model for the climate and biological datasets, we conducted a post-hoc examination of outlier detection and regime shifts. For outlier detection of black swan events, we implemented a method similar to that described in Anderson et al. (2017) and applied it to the climate and biology time series. This approach relies on first differencing the posterior trend mean estimates of the climate and biology trends, $\boldsymbol{x}_t - \boldsymbol{x}_{t-1}$ and then applies a normal density function to identify year-over-year changes that were unlikely to have arisen from a normal distribution (given the process variance). Probabilities can then be assigned to the deviations in each year (e.g., 'there is a 1:1000 chance of observing a deviation

288 similar to that estimated in year *t*'). As described in Ward et al. (2019), the presence of regimes
289 can also be estimated by applying hidden Markov models (HMM) to the estimated state indices
290 from a DFA. We evaluated support for regimes and alternate states by using the posterior trend
291 estimates from each model as input. The Bayesian Leave-One-Out cross validation Information
292 Criterion (LOOIC, Vehtari et al. 2017) was used to identify the data support for the number of
293 trends (n = 1–3).
294
295 *Forecasting community state*
296 While a wide variety of multivariate or univariate time series methods could be applied to our
297 observed time series to generate forecasts, our objectives were to develop simultaneous estimates
298 of both the community state(s) and the raw time series. We evaluated the ability of our DFA
299 models to generate short-term (one year lead-time) forecasts of community state by first
300 evaluating whether the performance of the biology DFA model was improved when climate time
301 series were included as covariates in the model. If climate time series were found to better
302 explain the variability in the biology time series, these relationships could potentially be used to
303 forecast community trends. For our analysis, we ran the DFA on a subset of the biology data
304 overlapping in time with the climate dataset, i.e., 1981–2017, to make out-of-sample predictions.
305 We used the same LFO-CV procedure described above, with the same forecast period (2009–
306 2017) to compare the biology models with and without a single climate covariate (see S2 Table
307 for all model formulations). In this case, the model used biological and climate data from all
308 preceding years and climate data from the year to be forecast. The six climate covariates from
309 the southern region and the central region of the CCE (12 total) were tested in this analysis. Once
310 the best-supported biology-covariate model was identified, we used that model to make

311 predictions of individual species parameters and the community state in 2018 using climate data
312 from that same year. We evaluated forecast skill based on the prediction errors of individual
313 species parameters and by comparing the forecasts for 2009–2018 to the 2009–2018 trend values
314 estimated from biology-covariate model that only included data prior to the forecast year.
315
316 **Results**
317 *Climate and biology trends*
318 The model with the highest predictive accuracy (ELPD) of the climate state in the southern and
319 central regions of the CCE was a one-trend DFA model (Model 1 in Table 1, Fig. 2a). This
320 model included unique observation variances across the six time series, support for heavy-tailed
321 deviations of the latent trend, an AR(1) coefficient on the trend (S1 Fig.), and an estimated trend
322 variance. All but one of the climate time series (central ILD) were associated with the single
323 trend, i.e., at least 90% of the loading posterior distributions associated with each time series
324 were above or below zero (Fig. 2b). The SST, SSH, and BV frequency (water column
325 stratification) time series from the southern and central regions of the CCE loaded positively on
326 this trend (Fig. 2b). The BEUTI and CUTI time series from both regions of the CCE and the ILD
327 time series from the central region loaded negatively on the trend (Fig. 2b). Overall, the trend
328 captured a well-documented cooling period in the CCE between 1980 and 2010 (e.g., Seo et al.
329 2012), as well as strong El Niño events (e.g., 1982–1983, 1997–1998, 2015–2016) and the 2014–
330 2016 marine heatwave. The trends and loadings indicate that these events were generally
331 associated with weaker upwelling, reduced mixed layer depth, low nutrient flux, and warm,
332 stratified waters (Fig. 2a, b).
333

Table 1. Summary information for climate and biology Bayesian DFA models, including whether process error was estimated, observation error variances (unequal or equal among time series, or unique to each survey), the number of model trends, expected log pointwise predictive densities (ELPD), and standard error of ELPD. Bold text highlights the models that show best support or highest predictive accuracy for the climate and biology data for the southern and central California Current ecosystem (i.e., highest ELPD). All climate and biology models include an AR(1) process and Student-t deviations.

Time series	Model	Process sigma	Variance index	Trends	ELPD	SE ELPD
Climate	1	Yes	unequal	1	**-10551.89**	759.44
	2	No	unequal	1	-10682.39	712.96
	3	Yes	equal	1	-16793.59	1732.54
	4	No	equal	1	-16881.03	1824.42
	5	No	unequal	2	-17441.01	1655.23
	6	Yes	unequal	2	-17818.86	1813.65
	7	Yes	unequal	3	-21571.65	1674.77
	8	No	unequal	3	-22882.99	1695.12
	9	No	equal	2	-23927.86	2694.72
	10	Yes	equal	2	-24536.19	2953.38
	11	Yes	equal	3	-38895.66	4024.93
	12	No	equal	3	-38920.87	4762.15
Biology	13	No	survey	1	**-2003.32**	95.76
	14	Yes	survey	1	**-2003.96**	88.88
	15	No	survey	2	-2155.52	76.05
	16	Yes	survey	2	-2198.79	78.86
	17	No	survey	3	-2334.55	118.31
	18	Yes	survey	3	-2335.10	112.70

Figure 2. Climate variability in southern and central California Current ecosystem: a) shared trend with 95% credible intervals (1981–2017), b) posterior distributions for loadings on all of the individual time series. Loadings with darker shading indicate time series loading most strongly on the climate trend. SST, sea surface temperature; SSH, sea surface height; ILD, isothermal layer depth; BV, Brunt-Väisälä frequency (stratification); CUTI, Coastal Upwelling

Transport Index; BEUTI, Biologically Effective Upwelling Transport Index. See S1 Table and S1 Figure for climate times series details.

The climate state during the marine heatwave, as indicated by the DFA trend, was within the bounds of previous observations. While there was support in the best model for heavy-tailed deviations in the climate trend (i.e., Student-t deviations S1 Fig.), our post-hoc examination of outliers detected a single extreme event in the climate state in mid-1998 to mid-1999 (threshold=0.001), when there was a shift from strong El Niño (1997–98) to strong La Niña (1998–1999) conditions, and not around the time of the heatwave. Application of the Bayesian HMM to the climate trend most supported the presence of two hidden states, reflecting the probability of being in a state associated with warmer conditions versus one with cooler conditions (LOOIC: one-state = 129.1, two-state = 9.4, three-state = 27.2, Fig. 3). The LOOIC did not provide support for a shift to a third novel climate state in the southern and central regions of the CCE during the marine heatwave, however there is a shift back to the previously observed warm state during the marine heatwave.

Figure 3. Results of Hidden Markov Models (HMM) showing state probability for latent trends in the climate (top) and biology (bottom) data sets. The best model for both data sets invoked two states, and the median probability (and 95% credible intervals) of being in one state versus the other is shown. The top figure reflects the probability of being in the state associated with warmer conditions versus one with cold conditions, and bottom figure indicates that ecosystem did not shift into a new state following the marine heatwave.

The best model for community variability among our biological time series was also a one trend model (Model 13 in Table 1, Fig. 4a). The model formulation was similar to the best climate model, except the observation variances were unique by dataset (survey) and not individual time series. We note that the top two models (Model 13 and 14) showed similar predictive accuracy (Δ ELPD < 1) and only differed with respect to whether the process variance was fixed at 1 or estimated. Here we only show results for the model with a fixed process variance. The biology showed strong coherence in community signal; a majority of the time series (31 of 38) loaded strongly (probability > 0.9) on the single trend and most of them demonstrated loadings in the same direction (Fig. 4b). The magnitude and direction of the estimated loadings were consistent with the observed high relative abundance of most juvenile groundfishes (rockfish, flatfish), squid, krill, and some ichthyoplankton species increased during the marine heatwave, and suggest that the reproductive success of some seabird species was higher around the time of the heatwave as well. The few time series loading in the other direction on the trend indicated a reduction in sea lion pup growth rate and lower abundances of juvenile/adult Pacific sardine *Sardinops sagax* and some ichthyoplankton species (e.g., larval northern anchovy and Pacific hake *Merluccius productus*) associated with the heatwave.

Figure 4. Community variability in the southern California Current ecosystem: a) shared trend with 95% credible intervals (1951–2018), b) posterior distributions for loadings on individual time series (only time series with ≥ 90% of the loading distributions above or below zero are shown). Loadings with darker shading indicate time series loading most strongly on the biology trend. Cal. = California, Juv. = juvenile fish stage, Juv./adult = juvenile and adult fish stages combined, all other fish are larval fish. See S1 Table and S1 Figure for times series details.

394

395 The estimated trend from this biology DFA model demonstrates a potential shift in community
396 state in the mid-1960s, although there is considerable uncertainty around the trend during this
397 early portion of the time series, likely due to the limited number of observations
398 (ichthyoplankton only) pre-dating the 1970s (Fig. 4a, S1 Fig.). Similarly, the limited number of
399 biological time series and missing sampling years in the late 1960s and 1970s, and the lack of
400 climate outputs from ROMS prior to 1980, make it difficult to detect a documented transition
401 that happened in the mid-1970s (S1 Fig., see discussion). The community state appears to be
402 relatively stable from the late 1970s through the early 2000s, and the trend reached a peak
403 around 2013–2015. Evidence of a community shift early in the time series is supported by our
404 regime detection analysis, which demonstrated that a two-state model best described the latent
405 trend (LOOIC: one-state = 216.4, two-state = 11.8, three-state = 41.8, Fig. 3). This shift
406 coincides with a strong increase in the abundance of a few species during that period, including
407 eared blacksmelt (*Lipolagus ochotensis*), slender blacksmelt (*Bathylagus pacificus*), northern
408 lampfish (*Stenobrachius leucopsarus*), as well as a rise in northern anchovy (*Engraulis mordax*)
409 abundance prior to the shift (S1 Fig.). Our analysis does not document a shift to a novel
410 community state in response to the recent marine heatwave.

411 While this model provided slight support for heavy-tailed Student-t deviations in the
412 latent trend (S2 Fig.), we did not detect any black swan events in the community state. We note
413 that the community response to two strong El Nino events (1982–1983 and 1997–1998) and to
414 unusually low productivity conditions (2005) in the central CCE appear similar in magnitude and
415 duration to the response to the 2014-2016 marine heatwave, although the directions of the
416 responses were opposite (Fig. 4a). Our regime detection analysis also captured the change in the

central CCE community in the mid to late 2000s (Fig. 3), which may be associated with the large changes in the reproductive success of multiple seabirds (e.g., Cassin's auklet, common murre, Brandt's cormorant) and in sea lion pup births around that time (S1 Fig). These taxa may have been impacted by changes in the abundance or availability of important prey items resulting from unproductive ocean conditions in the central CCE in 2005 and the below normal SSTs associated with the 2007-2008 La Nina Event (McClatchie et al. 2008, 2009, Bjorkstedt et al. 2010).

Forecast of community state

In comparing models of the biological response with and without climate covariates, we found that several biology models with climate predictors outperformed the biology models that did not include covariates (S2 Table). The climate covariate resulting in the best future predictions of community state was BEUTI (central region), followed by CUTI (central region) (Table 2, see S2 Table for all models). The coefficients linking BEUTI to observed time series (**B** matrix) indicate strong, positive relationships between nitrate flux and the reproductive success of seabirds and the abundance of krill in the central California Current (Fig. 5). They also indicate strong, negative relationships between nitrate flux and the abundance of juvenile/adult Pacific sardine and larval northern anchovy (Fig. 5). The remaining biology-BEUTI relationships were moderate (e.g., ichthyoplankton, market squid *Doryteuthis opalescens*) to weak (e.g., rockfish spp., Fig. 5). The biology-CUTI model was similar to the biology-BEUTI model with respect to model structure and estimated species loadings. The estimated coefficients in the CUTI model also show a similar pattern to those in the biology-BEUTI model (S5 Fig.). The remaining covariate models only showed weak climate-biology relationships (e.g., S5-S6 Fig.).

Table 2. Summary information for the top biology-covariate Bayesian DFA models for each covariate and the top two biology only models (years 1981-2017). The table indicates whether process error was estimated ('Yes') or fixed ('No'), the number of model trends, expected log pointwise predictive densities (ELPD), standard error of ELPD, the environmental covariate included in the model, and the region in the California Current over which the covariate was aggregated. All models had an AR(1) coefficient on the trend and Student-t deviations. Model 1 was deemed the best model based on its highest predictive accuracy (highest ELPD value) compared to all other models. BEUTI = Biologically Effective Upwelling Transport Index; BV = Brunt-Väisälä frequency; CUTI = Coastal Upwelling Transport Index; ILD = Isothermal Layer Depth; SST = Sea Surface Temperature; SSH = Sea Surface Height. See S2 table for the full suite of model comparisons.

Model	Process sigma	Trends	ELPD	SE ELPD	Covariate	Region
1	**No**	**1**	**-1878.71**	**71.52**	**BEUTI**	**central**
2	No	1	-1905.27	81.98	CUTI	central
3	No	1	-1914.62	83.22	ILD	south
4	No	1	-1927.33	88.26	SST	south
5	No	1	-1928.03	88.39	BV	south
6	No	1	-1946.75	86.33	SSH	south
7	No	1	-1951.44	73.59	None	-
8	Yes	1	-2038.71	91.44	None	-

Figure 5. A summary of the effect of the Biologically Effective Upwelling Transport Index (BEUTI), a measure of nitrate flux through the base of the mixed layer, on the single species parameters. Cal. = California, Juv. = juvenile fish stage, Juv./adult = juvenile and adult fish stages combined, all other fish are larval fish. Blue error bars reflect 95% credible intervals. Figures S4-S6 show effects of other environment covariates on the biological variables.

459

460 Given that the biology-BEUTI model was the best supported model over the null model
461 (a model without covariates), we were interested in evaluating the ability of this covariate model
462 to forecast the community state. Comparisons between the community state (out-of-sample
463 estimates) and the community state forecasts indicate that we had skill in forecasting community
464 state one year in advance (Fig. 6, S7 Fig., S8 Fig.). Forecasts of the community trend values for
465 nine additional years (2009–2017, S8 Fig.) also indicate that we had some skill for many of the
466 years tested. There are wide confidence intervals around the forecasts; however, given our
467 methodology we can expect that the credible intervals around the trend forecast will be larger
468 than the historical credible intervals (Fig. 6). Forecasts have more uncertainty than historical
469 values because the variance of a random walk increases linearly with time (Holmes 2004; Ward
470 et al. 2014). Furthermore, our credible intervals are increased because we are additionally (1)
471 propagating full parameter uncertainty across the MCMC draws projecting it, and (2) using a
472 Student-t distribution, which has heavy tails and therefore makes the uncertainty intervals wider
473 than if we used normal distribution.

474

475 **Figure 6.** Community variability and forecast of the community state in the southern California
476 Current. The shared biology trend (blue line, with 95% credible intervals) derived from biology-
477 BEUTI model fit to subset of data (1981–2018) is shown along with the trend forecast for 2018
478 (circle, with 95% credible intervals). See S7 Fig. for model loadings.

479

480 Overall, the model forecast skill of individual species parameters was moderate to high
481 for half of the species included in the biology-BEUTI model (S3 Table, S9 Fig.). It is important

to emphasize that the source of variability in predictions for each of the original time series is a mixture of the magnitude and uncertainty around the trends and loadings ($\boldsymbol{x}_t, \mathbf{Z}$), and the magnitude and uncertainty in the estimated covariates ($\boldsymbol{b}$). On the one hand, the time series associated with the highest predictive skill (i.e., lowest prediction errors) included seabird reproductive success (Common murre *Uria aalge*, Cassin's auklet *Ptychoramphus aleuticus*) and the abundance of juvenile Pacific sanddab *Citharichthys sordidus*, juvenile halfbanded rockfish *Sebastes semicinctus*, market squid, and several ichthyoplankton species (S3 Table, S9 Fig.). On the other hand, forecast skill was lowest (i.e., highest prediction errors) for the abundance of some juvenile rockfishes (chilipepper *Sebastes goodei* and widow rockfish *Sebastes entomelas*) and larval fishes (northern anchovy, mesopelagics), which is likely attributed to a lag or mismatch in the timing of the climate-biology relationships. These patterns in forecast skill are similar to those based on the biology-CUTI, -SST, and -ILD models (S3 Table). Lastly, the uncertainty around model predictions of species parameters appears to be driven more by the precision of the model coefficients than by the loadings on the community trend (e.g., S10 Fig.).

Discussion

We applied a novel set of statistical tools to data from the southern and central regions of the CCE to document the community response to climate perturbations over the past six decades and to create near-term forecasts of community state. Our analysis detected a community response to the 2014-2016 northeast Pacific marine heatwave; however, it did not exceed normal variability within the study timeframe or result in a shift to a novel community state, based on the biological time series investigated here. We identified relationships between community state and multiple climate variables, with nitrate flux through the base of the mixed layer having the strongest

correspondence with individual species time series and the shared trend in community variability. Moreover, we demonstrated skill in creating simultaneous one-year lead time forecasts of species responses and community state.

There have been several studies and anecdotal evidence of unexpected biological responses to the 2014–2016 northeast Pacific marine heatwave. Based on the biological time series included in our analysis, the broader CCE community demonstrated a response to the marine heatwave, i.e. the biology trend is higher over those years than in previous years. However, our results do not demonstrate a widespread community reorganization beyond the archetypal community structure of this recognizably dynamic ecosystem within the southern and central CCE in response to this event. Instead, the mean values for the shared trend in the biology time series, as well as for the shared climate trend, were within the range of previous observations. An unusual aspect of the 2014–2016 events, relative to past warming associated with El Niño or other low-productivity warm periods, was the very high abundance of young-of-year rockfish and anchovy (Santora et al. 2017, Thompson et al. 2019, Schroeder et al. 2019), which differed from most past warm events in which the abundance of these taxa was greatly reduced. There were many species present during the marine heatwave that are not typically observed in sampling or associated with the CCE, but those exceptional presences and high abundances of warm species did not result in a persistent signal among the species for which we have time series contributing to the DFAs. While our study did not detect a shift in community state in the southern and central CCE during the 2014–2016 heatwave, we did detect a shift in the 1960s. The 1960s shift was likely due to a regime shift previously detected in the southern California ichthyoplankton community (Peabody et al. 2018); the southern California ichthyoplankton time series are the only data used in our analysis that pre-date the 1970s.

528 Peabody et al. (2008) identified several species that caused the 1960s shift and their study
529 included a much broader suite of ichthyoplankton species than our study which limits our ability
530 to evaluate whether the species driving the shifts are consistent among studies. Previous studies
531 also documented a shift in response to the 1977/1978 PDO shift (e.g., McGowan et al. 2003,
532 Peabody et al. 2018) while our analyses did not. Our estimated biology trend is consistent with
533 the evidence of this regime shift, however, only ichthyoplankton time series are available prior to
534 the 1970s and there are gaps in the ichthyoplankton data between the late 1960s through the
535 1970s (CalCOFI only sampled every third year during this time). The trend estimate therefore
536 has higher uncertainty during this period than elsewhere in the time series. This likely limits any
537 detection of a regime shift in the mid to late 1970s. In a recent study, Litzow et al. (2020a)
538 applied Bayesian DFA to 11 climate time series and 48 biology time series in the Gulf of Alaska
539 (GOA). While their study revealed markedly elevated values in a shared climate trend between
540 2014–2019, it did not provide evidence of a shift to a novel mean state in shared trends of
541 ecosystem variability during the extreme warming event. Their analysis did, however, capture
542 the rapid community change in the GOA following the 1970's PDO shift in the northeast Pacific
543 Ocean. We note that our study, as well as Litzow et al. (2020a), are based on time series that
544 only extend a few years beyond the heatwave. As additional years of data become available, the
545 CCE and GOA Bayesian DFA models could reveal different outcomes. However, this is unlikely
546 given that the taxa and life stages used in both studies are known to respond quickly to changes
547 in ocean conditions, i.e., within less than one year, and given our assumption that the surveys are
548 consistently sampling at the right time and location to fully characterize the short-term response.
549 A compelling outcome of our analysis and the similar analysis of Alaskan species by
550 Litzow et al. (2020a) is that neither detected state changes in North Pacific communities

following the massive 2014-2016 marine heatwave, despite the extremely anomalous physical conditions throughout most of the basin and a litany of concurrent biological, ecological, social and economic effects (see Introduction). An important characteristic of both studies is the temporal scale of community analysis (1972-2017 for the GOA and 1951-2017 for the CCE). This long temporal scale provides an important context for comparing contemporary change with the magnitude of historical community shifts. In addition, the Bayesian DFA accounts for uncertainty in the shared trends in a way that prevents premature detection of wholesale ecosystem shifts. We note that Suryan et al. (2021), fitted a single-trend, non-Bayesian DFA model to a larger set of GOA biological time series (n = 187) over a shorter time span (2010-2018) and found evidence of a well-resolved shift that implied different community states during 2010-2014 and 2015-2018. The different conclusions of Suryan et al. (2021) and Litzow et al. (2020a) studies speak to an inherent tension in retrospective analyses of community change. Limited time series availability means that analyses can be taxonomically and functionally broad (e.g., Suryan et al. 2021), or temporally extensive (e.g., Litzow et al. 2020a), but not both. Each approach has advantages, but direct comparison between the two is difficult. Given the impacts of the 2014-2016 event, and that long-term warming combined with marine heatwaves will push the CCE into novel climate states, we must consider ecological mechanisms that might explain why these communities were apparently resilient to the marine heatwave, along with revisiting methodological details that could further clarify our results.

The CCE shared biology trend and loadings captured unexpected patterns in the community response to regional climate perturbations. The biology time series included in this study showed strong coherence in community signal in response to regional climate perturbations across multiple trophic levels, life-history strategies, and datasets. Most of the

biological time series loaded in the same direction on the shared trend, with only a few time series showing the opposite pattern. In addition, several species that are typically associated with cooler ocean conditions show increased relative abundances during the marine heatwave. For example, past studies have shown that high abundances of pelagic juvenile rockfish and groundfish, squid, and krill are associated with more southward transport in the California Current, and more subarctic source waters, with abundance far lower in years with more subtropical waters, which are often associated with El Niño and anomalous warm events (Ralston et al. 2015, Schroeder et al. 2019). Our analysis captured this documented pattern, showing a reduced abundance of these species that have been associated with subarctic source waters and strong equatorward flow in the California Current during two of the strongest El Nino events on record (1982–1983, 1997–1998) and unusually low productivity conditions (2005–2006, Peterson et al. 2006). Our analysis also captured the unexpected increase in abundance of these taxa in 2014–2016 despite the anomalously warm ocean conditions at that time. This may be partially explained by the observation that subsurface waters were more subarctic, rather than subtropical in origin (Schroeder et al. 2019) and that there was some strong upwelling during the marine heatwave, particularly in spring 2015 (Peterson et al. 2015, Ryan et al. 2017). The reduced production of juvenile/adult Pacific sardine and increase in juvenile northern anchovy between 2014 and 2016 shown here and elsewhere (Thompson et al. 2019) were consistent with a history of observations indicating that these species tend to respond asynchronously to ocean conditions (MacCall 1996, Schwartzlose et al. 1999, Chavez et al. 2003, Deyle et al. 2013, Sydeman et al. 2020). However, the responses were of opposite sign from past observations of increases in sardines and decreases in anchovy under warm conditions (Chavez et al. 2003). The DFA trends and loadings indicate a negative response of sea lion pup growth and weight to the

2014–2016 marine heatwave, which also aligns with past work showing that reduced prey availability for nursing mother sea lions is unfavorable for sea lion pups (McClatchie et al. 2016). Notably, sea lion pup condition covaried with abundance of anchovy and sardine, which provide quality prey to sustain lactation. Pup condition also improved at the tail end of the marine heatwave when, despite the warm water, anchovy abundance increased dramatically and by 2017 all metrics of pup condition were above average (Thompson et al. 2019). In addition, the trends and loadings suggest that the reproductive success of some seabirds in the central region of the CCE was not diminished by the heatwave, although recent studies have documented the severe impact of the heatwave on seabird productivity in regions to the north (Piatt et al. 2020). Our analysis is not able to capture the irruptions of fishes and invertebrates that are rare in long-term CCE time series. Many sporadically occurring taxa such as pelagic red crabs (*Pleuroncodes planipes*), which are absent from California waters in most years but abundant infrequently in warm years with anomalous transport from the south, are not well suited to include as time series due to large number of zero observations in the survey data.

Incorporating climate information in DFA models of CCE biology indicated that models with a climate covariate performed better than models without one. The model results suggest that nitrate flux into the surface mixed layer (BEUTI) was the best covariate for individual species in addition to the shared trend in the southern and central CCE over the past three decades. Nitrate flux had a strong positive effect on the abundance of krill and some larval fishes and on the reproductive success of seabirds, and a moderate positive effect on some pelagic juvenile fishes, squid, and sea lion pup births. Stronger upwelling magnitude (CUTI), which is correlated with nitrate flux, was the second-best predictor of community variability and had a positive albeit weaker effect on the same suite of species (S4 Fig.). These findings are consistent

620 with mechanistic understanding as upwelling increases the supply of nutrients from deep to
621 shallow waters and enhances the productivity at the lower trophic levels that affect foraging
622 conditions for higher trophic level species in coastal habitats. For example, past work has shown
623 that rockfish abundance is positively associated with upwelling strength (Ralston et al. 2013),
624 and seabird productivity has been shown to increase when ocean conditions support high primary
625 production and higher trophic level prey (e.g. Wells et al. 2008). Rockfish production is also
626 higher when subsurface source waters in the California Current are more subarctic rather than
627 subtropical, which may explain the negative effect of isothermal layer depth (ILD) and
628 temperature on some rockfish species (S5 Fig., S6 Fig.). More subtropical source waters and
629 surface warming tend to be associated with deeper isopycnals, higher stratification, and
630 shallower ILD (Schroeder et al. 2019, Bograd et al. 2019). Nitrate flux (BEUTI) had a strong
631 negative correlation with juvenile/adult Pacific sardine and larval northern anchovy and
632 upwelling strength (CUTI) did as well. The relative abundance of Pacific sardine in coastal
633 waters off of Central California has been shown to be lower during periods of strong upwelling
634 (Santora et al. 2014, Ralston et al. 2015). This trend may reflect a change in the production of
635 Pacific sardine or a shift in their relative distribution. In addition, a negative relationship between
636 upwelling and nitrate flux and sardine recruitment can generally be explained by the transfer of
637 fish larvae to offshore areas where they have low chance of survival during periods of strong
638 equatorward flow and upwelling (Bailey and Francis 1985, Nieto et al. 2014), although our
639 understanding of the mechanisms driving anchovy population dynamics is limited (Sydeman et
640 al. 2020). We acknowledge that climate drivers often act in concert to influence community
641 variability, and here we are evaluating the effects of the climate variables one at a time. An
642 important next step of this work will be to examine whether including multiple climate

643 covariates in the CCE biology model further improves the forecast skill of the model and our
644 community state indicator. However, the individual climate variables are collinear and share
645 information, which affects our ability to makes inference on the covariates. Furthermore, our
646 study is an attempt to synthesize a broader suite of community indicators and their response to
647 climate perturbations and therefore should not be interpreted as replacing or simplifying more
648 detailed investigations into the drivers and mechanistic understanding of the indicators included
649 here.

650 Our approach for creating simultaneous predictions of species responses and shared
651 ecosystem variability to ocean conditions shows promise for developing near-term forecasts of
652 community state. Our forecasts are based on ocean model data derived from the CCE ROMS,
653 which have been applied in several recent studies to examine how oceanographic processes
654 affect fish recruitment variability (Tolimieri et al. 2018, Haltuch et al. 2020) and productivity
655 (Siegelman-Charbit et al. 2016), species habitat suitability (Abrahms et al. 2018, Cimino et al.
656 2020), and species spatial distributions (Muhling et al. 2019, 2020). The CCE ROMS also
657 supports nowcasts of species distributions based on observed ocean conditions that can help
658 resource managers and users manage risks associated with fisheries bycatch and ship-strike
659 (Hazen et al. 2017, 2018, Welch et al. 2019). Moreover, multiple efforts are underway in the
660 CCE and other coastal systems to develop short-term forecasts (1–24 months) of ocean
661 conditions for uptake by scientists, managers, and other end-users (Siedlecki et al. 2016, Kaplan
662 et al. 2016, Jacox et al. 2020, Malick et al. 2020). Here, we were able to create forecasts of
663 community state and several individual species parameters one year in advance based on
664 observations of a single climate variable (nitrate flux). The lead-time of such a forecast could be
665 extended further by using forecasts of ocean conditions rather than observed conditions, and

ocean temperatures in the CCE can be skillfully forecast months to a year in advance, with particularly high skill in the late winter and spring (Jacox et al. 2019). As mentioned above, future extensions of our work will evaluate whether a combination of climate variables as well as time lags might improve our forecasting skill.

In the CCE, nonstationary relationships are an important consideration for producing reliable ecological forecasts in this ecosystem. While the year-to-year variability in the estimated trend did appear to be stationary for our community models (Fig. 4, 6), the autocorrelation appeared to be nonstationary with the lag-1 autocorrelation between 2000–present being significantly higher (0.82) than over the years 1981–2000 (0.23). In addition to nonstationary variance parameters, future analyses may also consider nonstationary relationships in the covariate relationships, or potential interactions between covariates. A growing number of retrospective analyses have revealed nonstationary relationships among climate and individual species or community-level variables (Puerta et al. 2019, Litzow et al. 2018, 2019, 2020 a,b,c). In the northeast Pacific Ocean, these studies have been mostly focused on Alaskan ecosystems, which have long time series that support robust statistical analysis of nonstationarity in climate and biological systems. The best-documented instance of nonstationary relationships among climate and biology time series in the North Pacific centers on a climate shift in the late 1980s (Litzow et al. 2020b). Decades of observational data on either side of that event allow for statistically robust tests for nonstationarity that are not yet available for post-2014–2016 conditions. The problem of having few years of available data is an inescapable limitation for evaluating the possibility that nonstationary relationships might accompany emerging, novel climate conditions. Similarly, the considerable historical and paleoceanographic evidence for low frequency variability in the productivity of many key marine populations, particularly coastal

689 pelagic species such as Pacific sardine and northern anchovy, also complicates the challenges
690 associated with detecting nonstationarity with data of a limited temporal duration (Baumgartner
691 et al. 1992, MacCall 1996, Field et al. 2009), although such patterns may lead to greater risk of
692 "detecting" nonstationarity when in fact it may not exist (Cohn and Lins 2005, Milly et al. 2015).
693 However, early indications from Alaska suggest the possibility that long-standing relationships
694 between leading climate modes and individual climate and biology time series may have
695 changed following 2014 (Litzow et al. 2020c).

696 Using DFA to forecast attributes of community structure in the CCE allows us to create
697 simultaneous forecasts of trends, or 'ecosystem state', and raw time series. This approach could
698 also be applied individually to each dataset in our analysis to generate taxa-specific indicators
699 (e.g., seabird productivity, juvenile fish abundance), though forecasts would be expected to differ
700 from those with the entire CCE data. Similarly, if ecosystem states were not a focus of inference,
701 alternative forecast models could be applied (e.g., ARIMA or non-parametric models, Ward et al.
702 2014). Forecasts for individual time series from the DFA models used here can be seen as a
703 mixture of the AR forecast on the estimated trends (Fig. 6), and linear effects of forecasted
704 climate variables on each time series (Fig. 5). Species that have strong associations or loadings
705 on the trend and estimated climate effects that are large in magnitude (e.g., market squid, Pacific
706 sanddabs, shortbelly rockfish *Sebastes jordani*) are expected to have the most accurate
707 predictions, while those species with weak loadings and weaker effects of climate variables (e.g.,
708 California smoothtongue (*Leuroglossus stilbius*) are expected to have worse forecast
709 performance.

710 Our approach for developing a community state indicator to track and predict the
711 response of marine ecosystems to climate perturbations has the potential to support ecosystem-

based and climate-ready management in multiple ways. Garnering knowledge of community state and the potential for large shifts in ecosystem structure in response to intense and novel climate perturbations can help inform better, more rapid management decisions for mitigating ecological and socioeconomic impacts. The combination of long-term monitoring surveys and data with the modeling framework we advance here can also help scientists identify or refine key variables of ecosystem change that are summarized for ecosystem assessments in support of decision-making (Harvey et al. 2020). For example, it might be prudent to emphasize ecological time series that load strongest on ecosystem state trends and demonstrate strong, predictable relationships with climate variables (or other covariates of interest) over time series with weaker loadings on shared trends of community variability or have low forecast skill with environmental variables. Furthermore, our approach can provide valuable ecosystem information for scientific, management and coastal communities during times when researchers cannot sample the biology in marine ecosystems. This added value became acutely apparent in 2020 when myriad ocean surveys were cancelled or limited in spatiotemporal scope due to safety restrictions associated with the COVID-19 pandemic. Finally, our approach provides a quantitative way to help managers discern short-term periods of unusual community dynamics and/or high variability—such as the 2014-2016 marine heatwave—from state shifts that represent more enduring transitions into new regimes of ecosystem structure or productivity. Given that global climate change is expected to amplify ocean change, approaches like the one applied here will become increasingly valuable for marine resource management and conservation.

Acknowledgements

We thank those who have spent countless hours planning field surveys and collecting data for the invaluable time series used in our study. We thank the U.S. Fish and Wildlife Service for granting permission and providing resources to conduct research on the Farallon Islands National Wildlife Refuge. Funders for Point Blue's Farallon Research Program include the Bently Foundation, Elinor Patterson Baker Trust, Bernice Barbour Foundation, Frank A. Campini Foundation, Grand Foundation, Kimball Foundation, Marisla Foundation, Giles W. and Elise G. Mead Foundation, Moore Family Foundation, RHE Charitable Foundation, Volgenau Foundation, and numerous individual donors. We thank B. Feist for creating the map of the sampling areas (Figure 1). We thank N. Tolimieri and T.L. Rogers for their helpful comments that improved this manuscript. Funding for this project came from NOAA's Fisheries and the Environment (FATE) program (project 16-01) and NOAA's California Current Integrated Ecosystem Assessment program.

References

Abrahms B, Welch H, Brodie S, Jacox MG, Becker EA, Bograd SJ et al. Dynamic ensemble models to predict distributions and anthropogenic risk exposure for highly mobile species. Divers. Distrib. 2019; 25: 1182-1193. doi: 10.1111/ddi.12940.

Anderson SC, Ward EJ. Black swans in space: modelling spatiotemporal processes with extremes. Ecology 2019; 100: e02403. doi:10.1002/ecy.2403.

Anderson SC, Branch TA, Cooper AB, Dulvy NK. Black-swan events in animal populations. Proc. Natl. Acad. Sci. U.S.A. 2017; 114: 3252–3257.

Anderson PJ. Piatt JF. 1999. Community reorganization in the Gulf of Alaska following ocean climate regime shift. Mar. Ecol. Prog. Ser. 1999; 189: 117-123.

Bailey KM, Francis RC. Recruitment of Pacific Whiting, Merluccius productus, and the ocean environment. Mar. Fish. Rev. 1985; 47: 8-11.

Baumgartner TR, Soutar A, Ferreira-Bartrina V. Reconstructions of the history of Pacific sardine and northern anchovy populations over the past two millennia from sediments of the Santa Barbara Basin, California. CalCOFI Rep. 1992; 33: 24-40.

Beaugrand G, Edwards M, Brander K, Luczak C, Ibanez F. Causes and projections of abrupt climate-driven ecosystem shifts in the North Atlantic. Ecol. Lett. 2008; 11: 1157–1168.

Beaugrand G, Conversi A, Chiba S, Edwards M, Fonda-Umani S, Greene C et al. Synchronous marine pelagic regime shifts int he Northern Hemisphere. Phil. Trans. R. Soc. 2016; 370: 20130272. doi: 10.1098/rstb.2013.0272.

Benson AJ, Trites AW. Ecological effects of regime shifts in the Bering Sea and eastern North Pacific Ocean. Fish Fish. 2002; 3: 95–113.

Bjorkstedt EP, Goericke R, McClatchie S, Weber E, Watson W, Lo N et al. State of the California current 2009-2010: Regional variation persists through transition from the la Niña to el Niño (and back?). CalCOFI Rep. 2010; 51.

Bograd S, Schroeder ID, Jacox MG. 2019. A water mass history of the Southern California current system. Geophys. Res. Lett. 2019; 46: 6690-6698.

Bond NA, Cronin MF, Freeland H, Mantua N. Causes and impacts of the 2014 warm anomaly in the NE Pacific. Geophys. Res. Lett. 2015; 42, 3414–3420. doi: 10.1002/2015GL063306.

Bürkner P-C, Gabry J, Vehtari A. 2020. Approximate leave-future-out cross-validation for Bayesian time series models. J. Stat Comput. Simul. 2020; 90: 2499-2523.

Brodeur RD, Auth TD, Phillips AJ. Major shifts in pelagic micronekton and zooplankton community structure in an upwelling ecosystem related to an unprecedented marine

heatwave. Front. Mar. Sci. 2019. doi: 10.3389/fmars.2019.00212.

Carpenter B, Gelman A, Hoffman MD, Lee D, Goodrich B, Betancourt M et al. Stan: A Probabilistic Programming Language. J. Stat. Softw. 2017. doi: 0.18637/jss.v076.i01.

Cavole LM, Demko AM, Diner RE, Giddings A, Koester I, Pagniello CM et al. Biological impacts of the 2013–2015 warm-water anomaly in the Northeast Pacific: winners, losers, and the future. Oceanography 2016; 29, 273–285.

Chavez FP, Ryan J, Lluch SE, Niquen MC. From Anchovies to Sardines and Back: Multidecadal change in the Pacific Ocean. Science 2003; 299: 217-221.

Cimino MA, Santora JA, Schroeder I, Sydeman W, Jacox MG, Hazen EL, Bograd SJ. Essential krill species habitat resolved by seasonal upwelling and ocean circulation models within the large marine ecosystem of the California Current System. Ecography 2003; 43, 1-15. doi: 10.1111/ecog.05204.

Cohn TA, Lins, HF. Nature's style: Naturally trendy. Geophys. Res. Lett. 2005. doi: 10.1029/2005GL024476

Deyle ER, Fogarty M, Hsieh C-h, Kaufman L, MacCall AD, Munch SB et al. Predicting climate effects on Pacific sardine. Proc Natl Acad Sci USA 2013; 110: 6430-6435.

Field DB, Baumgartner TR, Ferreira V, Gutierrez D, Lozano-Montes H, Salvatteci R, Soutar A. Variability from scales in marine sediments and other historical records. In: Checkley DM, Alheit J, Oozeki Y, editors. Climate change and small pelagic fish. Cambridge: Cambridge University Press; 2009. pp. 45-63.

Field JC, Miller RA, Santora JA, Tolimieri N, Haltuch MA, Brodeur RD et al. Spatiotemporal patterns of variability in the abundance and distribution of winter-spawned pelagic juvenile rockfish in the California Current. PloS one 2021; 16: e0251638.

Gelman A, Carlin JB. Stern HS, Dunson DB, Vehtari A, Rubin DB. Bayesian Data Analysis. 3rd ed. CRC Press; 2013.

Gelman A, Rubin DB. Inference from Iterative Simulation Using Multiple Sequences. Statist. Sci. 1992; 7: 457-472.

Haltuch MA, Tolimieri N, Lee Q, Jacox MG. Oceanographic drivers of petrale sole recruitment in the California Current Ecosystem, Fish. Ocean. 2020; 29:122-136. doi: 10.1111/fog.12459.

Hare SR, Mantua NJ. Empirical evidence for North Pacific regime shifts in 1977 and 1989. Prog. Oceanogr. 2000; 47: 103–145. doi: 10.1016/s0079-6611(00)00033-1.

Harvey CJ, Fisher J, Samhouri, JF, Williams GD, Francis TB, Jacobson KC et al. The importance of long-term ecological time series for integrated ecosystem assessment and ecosystem-based management. Prog. Oceanogr. 2020. doi: 10.1016/j.pocean.2020.102418.

Hazen EL, Palacios DM, Forney KA, Howell EA, Becker E, Hoover AL et al. WhaleWatch: a dynamic management tool for predicting blue whale density in the California Current. J. Appl. Ecol. 2017. doi: 10.1111/1365-2664.12820.

Hazen EL, Scales KL, Maxwell SM, Briscoe D, Welch, H, Bograd et al. A dynamic ocean management tool to reduce bycatch and support sustainable fisheries. Sci. Adv. 2018, 4: eaar3001.

Hobday AJ, Oliver ECJ, Sen Gupta A, Benthuysen JA, Burrows MT, Donat MG et al. Categorizing and naming marine heatwaves. Oceanography 2018; 31: 162 - 173.

Hobday AJ, Spillman CM, Paige Eveson J, Hartog JR. Seasonal forecasting for decision support in marine fisheries and aquaculture. Fish. Oceanogr. 2016; 25: 45–56.

Hoffman MD, Gelman A. The No-U-Turn Sampler: Adaptively Setting Path Lengths in

826 Hamiltonian Monte Carlo. J. Mach. Learn. Res. 2014; 15: 1593–1623.
827 Holmes EE. Beyond theory to applications and evaluation: Diffusions approximations for
828 population viability analysis. Ecol. Appl. 2004; 14: 1272-1293.
829 Holmes EE, Ward EJ, Scheuerell, MD. Analysis of multivariate time series using the MARSS
830 package; 2018.
831 Jacox MG, Alexander MA, Siedlecki S, Chen K, Kwon Y-O, Brodie S et al. Seasonal-to-
832 interannual prediction of North American coastal marine ecosystems: Forecast methods,
833 mechanisms of predictability, and priority developments. Prog. Oceanogr. 2020. doi:
834 10.1016/j.pocean.2020.102307.
835 Jacox MG, Alexander MA, Stock CA, Hervieux G. On the skill of seasonal sea surface
836 temperature forecasts in the California Current System and its connection to ENSO
837 variability. Clim. Dyn. 2019; 53: 7519-7533.
838 Jacox MG, Alexander MA, Mantua NJ, Scott JD, Hervieux G. Webb RS et al. Forcing of
839 multiyear extreme ocean temperatures that impacted California Current living marine
840 resources in 2016. Bull. Am. Meteorol. Soc. 2018a; 99: S27–S33. doi: 10.1175/BAMS-D-
841 17-0119.1
842 Jacox MG, Edwards CA, Hazen EL, Bograd, SJ. Coastal upwelling revisited: Ekman, Bakun,
843 and improved upwelling indices for the U.S. west coast. J. Geophys. Res. 2018b.
844 doi:10.1029/2018JC014187.
845 Jones T, Parish JK, Peterson WT, Bjorkstedt EP, Bond NA, Balance LT et al. Massive mortality
846 of a planktivorous seabird in response to a marine heatwave. Geophys. Res. Lett. 2018; 45:
847 3193-3202.
848 Kaplan IC, Williams GD, Bond NA, Hernmann AJ, Siedlecki S. et al. Cloudy with a chance of

849 sardines: forecasting sardine distributions using regional climate models. Fish. Oceanogr.
850 2016; 25: 15-2.
851 Koslow J, Goericke R, Watson W. Fish assemblages in the Southern California Current:
852 relationships with climate, 1951–2008. Fish. Oceanogr. 2013; 22: 207–219.
853 Koslow JA, Hobday AJ, Boehlert GW et al. Climate variability and marine survival of coho
854 salmon (*Oncorhynchus kisutch*) in the Oregon production area. Fish. Oceanogr. 2002; 11: 65-
855 77.
856 Laufkötter C, Zscheischler J, Frölicher TL. High-impactmarine heatwaves attributable to human-
857 induced global warming. Science 2020; 369: 1621-1625.
858 Litzow MA, Ciannelli L. 2007. Oscillating trophic control induces community reorganization in
859 a marine ecosystem. Ecol. Lett. 2007; 10: 1124–1134. doi: 10. 1111/j.1461-
860 0248.2007.01111.x.
861 Litzow MA, Ciannelli L, Puerta P, Wettstein JJ, Rykaczewski RR, Opiekun M. Non-stationary
862 climate–salmon relationships in the Gulf of Alaska. Proc. R. Soc. B Biol. Sci. 2018; 285:
863 20181855. doi: 10.1098/rspb.2018.1855.
864 Litzow MA, Ciannelli L, Puerta P, Wettstein JJ, Rykaczewski RR, Opiekun M. Nonstationary
865 environmental and community relationships in the North Pacific Ocean. Ecology 2019; 100:
866 ecy.2760. doi: 10.1002/ecy.2760.
867 Litzow et al. 2020a. Evaluating ecosystem change as Gulf of Alaska temperature exceeds the
868 limits of preindustrial variability. Prog. Ocean. 2020a; 117: 7665-7671.
869 Litzow MA, Hunsicker ME, Bond NA, Burke BJ, Cunningham CJ, Gosselin JL, Norton EL,
870 Ward EJ, Zador SG. 2020b. The changing physical and ecological meanings of North Pacific
871 Ocean climate indices. Proc. Natl. Acad. Sci. U.S.A. 2020b; 117: 7665–7671. doi:

872 10.1073/pnas.1921266117.
873 Litzow MA, Malick MJ, Bond NA, Cunningham CJ, Gosselin JL, Ward EJ. 2020c. Quantifying
874 a novel climate through changes in PDO-climate and PDO-salmon relationships. Geophys.
875 Res. Lett. 2020b. doi: 10.1029/2020GL087972.
876 MacCall AD. Patterns of low-frequency variability in fish populations of the California Current.
877 CalCOFI Reports 1996; 37: 100-110.
878 Malick M.J, Siedlecki SA, Norton EL, Kaplan IC, Haltuch MA, Hunsicker ME et al. 2020.
879 Environmentally driven seasonal forecasts of Pacific hake distribution. Front. Mar. Sci. 7:
880 578490. doi: 10.3389/fmars.2020.578490.
881 Mantua NJ, Hare SR, Zhang Y, Wallace JM, Francis RC. A Pacific interdecadal climate
882 oscillation with impacts on salmon production. Bull. Am. Meteorol. Soc. 1997; 78, 1069–
883 1079.
884 McCabe RM, Hickey BM, Kudela RM, Lefebvre KA, Adams NG, Bill BD et al. An
885 unprecedented coastwide toxic algal bloom linked to anomalous ocean conditions. Geophys.
886 Res. Lett. 2016; 43: 10366–10376. doi:10.1002/2016GL070023.
887 McClatchie S, Goericke R, Koslow JA, Schwing FB, Bograd SJ, Charter R, W et al. The State of
888 the California Current, 2007–2008: La Niña conditions and their effects on the ecosystem.
889 Cal-COFI Rep. 2008; 49: 39–76.
890 McClatchie S, Goericke R, Schwing FB, Bograd SJ, Peterson WT, Emmett R et al. The state of
891 the California Current, 2008–2009: Cold conditions drive regional difference. CalCOFI
892 Rep. 2009; 50: 43–68
893 McClatchie S, Field J, Thompson AR, Gerrodette T, Lowry M, Fiedler PC et al. Food limitation
894 of sea lion pups and the decline of forage off central and southern California. R. Soc.

opensci. 2016; 3: 150628. doi: 10.1098/rsos.150628.

McGowan JA, Bograd SJ, Lynn RJ, Miller AJ. The biological response to the 1977 regime shift in the California Current. Deep Sea Res. II 2003; 50: 2567-2582.

Milly PCD, Betancourt J, Falkenmark M, Hirsch, RM, Kundzewicz ZW, Lettenmaier DP et al. On critiques of "Stationarity is dead: Whither water management?" Water Res. Res. 2015; 51: 7785–7789.

Möllmann C, Diekmann R. Marine Ecosystem Regime Shifts Induced by Climate and Overfishing: A Review for the Northern Hemisphere. Adv. Ecol. Res. 2012; 47: 303.347.

Morgan CA, Beckman BR, Weitkamp LA, Fresh KL. Recent ecosystem disturbance in the Northern California Current. Fisheries 2019; 44: 465-474. doi: 10.1002/fsh.10273.

Muhling B, Brodie S, Jacox MG, Snodgrass O, Dewar H, Tommasi D, Edwards C, Xu Y, Snyder S, Childers J. Dynamic habitat use of albacore and their primary prey species in the California Current System. CalCOFI Reports 2019; 60: 79-93.

Muhling B, Brodie S, Smith JA, Tommasi D, Gaitan CF, Hazen EL et al. Predictability of species distributions deteriorates under novel environmental conditions in the California Current System. Front. Mar. Sci. 2020; doi:10.3389/fmars.2020.00589.

Neveu E, Moore AM, Edwards CA, Fiechter J, Drake P, Jacox MG, Nuss E. A historical analysis of the California Current using ROMS 4D-Var. Part I: System configuration and diagnostics, Ocean Model. 2016; 99: 133-151. doi:10.1016/j.ocemod.2015.11.012.

Nielsen JM, Rogers LA, Brodeur RD, Thompson AR, Auth TD, Dreary AL et al. Responses of ichthyoplankton assemblages to the recent marine heatwave and previous climate fluctuations in several Northeast Pacific marine ecosystems. Glob. Chang. Biol. 2020; 27: 506-520.

Nieto K, McClatchie S, Weber ED, Lennert-Cody CE. Effect of mesoscale eddies and streamers on sardine spawning habitat and recruitment success off Southern and central California, J. Geophys. Res. Oceans 2014; 119: 6330–6339, doi:10.1002/014JC010251.

Peabody CE, Thompson AR, Sax DF, Morse RE, Perretti CT. Decadal regime shifts in southern California's ichthyoplankton assemblage. Mar. Ecol. Prog. Ser. 2018; 607: 71-83.

Peterson WT, Emmett R, Goericke R, Venrick E, Mantyla A, Bograd S et al. The State of the California Current, 2005-2006: warm in the north, cool in the south. CalCOFI Reports 2006; 47: 30–74.

Peterson et al. 2015 https://agupubs.onlinelibrary.wiley.com/doi/full/10.1002/2017JC012952

Piatt JF, Parrish JK, Renner HM, Schoen SK, Jones TT, Arimitsu ML et al. Extreme mortality and reproductive failure of common murres resulting from the northeast Pacific marine heatwave of 2014-2016. PLoSONE 2020; 15: e0226087. doi: 10.1371/journal.pone.0226087

Planque B, Arneberg P. 2018. Principal component analyses for integrated ecosystem assessments may primarily reflect methodological artefacts. ICES J. Mar. Sci. 2018; 75: 1021–1028.

Puerta P, Ciannelli L, Rykaczewski R, Opiekun M, Litzow MA. Do Gulf of Alaska fish and crustacean populations show synchronous non-stationary responses to climate? Prog. Oceanogr. 2019; 175: 161–170. doi: 10.1016/j.pocean.2019. 04.002.

R Core Team. R: A language and environment for statistical computing. R Foundation for Statistical Computing, Vienna, Austria, 2021.

Ralston S, Sakuma KM, Field JC. Interannual variation in pelagic juvenile

941 rockfish (Sebastes spp.) abundance – going with the flow. Fish. Ocean. 2013; 22:288–308.
942 doi: 10.1111/fog.12022.
943 Ralston S, Field JC, Sakuma KM. Long-term variation in a central Californiapelagic forage
944 assemblage. J. Mar. Sys. 2015; 146: 26-37. doi: 10.1016/j.jmarsys.2014.06.013.
945 Ryan JP, Kudela RM, Birch JM, Blum M, Bowers HA, Chavez FP et al. Causality of an extreme
946 harmful algal bloom in Monterey Bay, California, during the 2014–2016 northeast Pacific
947 warm anomaly. Geophys. Res. Lett. 2017; 44: 5571-5579. doi: 10.1002/2017GL072637.
948 Sakuma KM, Field JC, Mantua NJ, Ralston S, Marinovic BB, Carrion CN.
949 Anomalous epipelagic micronekton assemblage patterns in the neritic waters of the
950 California Current in spring 2015 during a period of extreme ocean conditions. CalCOFI
951 Reports 2016; 57: 163-183.
952 Sanford E, Sones JL, García-Reyes M, Goddard JH, Largier JL. Widespread shifts in the coastal
953 biota of northern California during the 2014–2016 marine heatwaves. Sci. Rep. 2019; 9: 1-
954 14.
955 Santora JA, Mantua NJ, Schroeder ID, Field JC, Hazen E, Bograd SJ et al. Habitat compression
956 and ecosystem shifts as potential links between marine heatwave and record whale
957 entanglements. Nat. Commun. 2020; 11: 1-12.
958 Santora JA, Hazen EL, Schroeder ID, Bograd SJ, Sakuma KM, Field JC. Impacts of ocean
959 climate variability on biodiversity of pelagic forage species in an upwelling ecosystem.
960 Mar. Ecol. Prog. Ser. 2017; 580: 205-220.
961 Santora JA, Schroeder ID, Field JC, Wells BK, Sydeman WJ. 2014. Spatiotemporal
962 dynamics of ocean conditions and forage taxa reveals regional structuring of predator-prey
963 relationships. Ecol. Appl. 2014; 24:1730-1747. doi:10.1890/13-1605.1.

964 Schroeder ID, Santora JA, Bograd SJ, Hazen EL, Sakuma, KM, Moore AM et al. Source water
965 variability as a driver of rockfish recruitment in the California Current Ecosystem:
966 implications for climate change and fisheries management. Can. J. Fish. Aquat. Sci. 2019;
967 76: 950-960. doi: 10.1139/cjfas-2017-0480.
968 Schwartzlose RA, Alheit J, Bakun A, Baumgartner TR, Cloete R, Crawford RJM et al. 1999.
969 Worldwide large-scale fluctuations of sardine and anchovy populations. S. Afr. J. Mar. Sys.
970 1999; 21: 289-347.
971 Sen Gupta A, Thomsen M, Benthuysen JA. *et al*. Drivers and impacts of the most extreme
972 marine heatwaves events. Sci. Rep. 2020; 10: 19359. doi: 10.1038/s41598-020-75445-3.
973 Seo H, Brink KH, Dorman E, Koracin D, Edwards CA. What determines the spatial pattern in
974 summer upwelling trends on the US West Coast? J. Geophys. Res. Oceans 2012. doi:
975 10.1029/2012JC008016.
976 Siedlecki SA, Kaplan IC, Hermann AJ, Nguyen TT, Bond NA, Newton JA et al. Experiments
977 with seasonal forecasts of ocean conditions for the northern region of the California
978 Current upwelling system. Sci. Rep. 2016; 6: 27203. DOI: 10.1038/srep27203.
979 Siegelman-Charbit L, Koslow JA, Jacox MG, Hazen EL, Bograd SJ, Miller EF, McGowan JA.
980 Physical forcing on fish abundance in the southern California Current System. Fish. Ocean.
981 2018; 27: 475–488. doi:10.1111/fog.12267.
982 Stan Development Team. RStan: The R interface to Stan. 2018.
983 Sydeman WJ, Dedman S, Garcia-Reyes M, Thompson SA, Thayer JA, Bakun A, MacCall AD.
984 Sixty-five years of northern anchovy population studies in the southern California Current: a
985 review and suggestion for sensible management. ICES J. Mar. Sci. 2020; 77: 486–499.

986 Thompson AR, Hyde JR, Watson W, Chen DC, Guo LW. Rockfish assemblage structure and
987 spawning locations in southern California identified through larval sampling. Mar. Ecol.
988 Prog. Ser. 2016; 547: 177-192.
989 Thompson AR, Schroeder ID, Bograd SJ, Hazen EL, Jacox MG, Leising AL et al. State of the
990 California Current 2018-19: a novel anchovy regime and a new marine heatwave?
991 CalCOFI Reports 2019; 60: 1-65.
992 Tolimieri N, Haltuch M, Lee Q, Jacox MG, Bograd SJ. Oceanographic drivers of sablefish
993 recruitment in the California Current. Fish. Ocean, 2018; 27: 458-474,
994 doi:10.1111/fog.12266.
995 Tommasi D, Stock CA, Hobday AJ, Methot R, Kaplan IC, Eveson JP et al. Managing living
996 marine resources in a dynamic environment: the role of seasonal to decadal climate
997 forecasts. Prog. Oceanogr. 2017; 152: 15–49.
998 Vehtari A, Gelman A, Gabry J. Practical Bayesian model evaluation using leave-one-out cross-
999 validation and WAIC. Statistics and Computing 2017; 27: 1413-1432. doi:
1000 10.1007/s11222-016-9696-4.
1001 Walker Jr HJ, Hastings PA, Hyde JR, Lea RN, Snodgrass OE, Bellquist LF. Unusual occurrences
1002 of fishes in the Southern California Current System during the warm water period of 2014–
1003 2018. Estuar. Coast. Shelf Sci. 2020; 236: 106634.
1004 Walsh JE, Thoman RL, Bhatt US, Bieniek PA, Brettschneider B, Brubaker M et al. The high
1005 latitude heat wave of 2016 and its impacts on Alaska. Bull. Am. Meteorol. Soc. 2018; 99:
1006 S39–S43. doi: 10.1175/BAMS-D-17-0105.
1007 Ward EJ, Holmes EE, Thorson JT, Collen B. Complexity is costly: a meta-analysis of parametric
1008 and non-parametric methods for short-term population forecasting. Oikos 2014; 123: 652-

661.

Ward EJ, Anderson SC, Damiano LA, Hunsicker ME, Litzow MA. Modeling regimes with extremes: the bayesdfa package for identifying and forecasting common trends and anomalies in multivariate time-series data. R J 2019; 11: 46–55.

Ward EJ, Anderson SC, Damiano LA, Malick MJ. bayesdfa: Bayesian Dynamic Factor Analysis (DFA) with 'Stan'. R package version 1.1.0 2020. https://CRAN.R-project.org/package=bayesdfa

Welch H, Hazen EL, Briscoe DK, Bograd SJ, Jacox MG, Eguchi T et al. Environmental indicators to reduce loggerhead turtle bycatch offshore of Southern California. Ecol. Ind. 2019; 98: 657-664. doi:10.1016/j.ecolind.2018.11.001.

Wells BK, Field JC, Thayer JA, Grimes CB, Bograd SJ, Sydeman WJ et al. Untangling the relationships among climate, prey and top predators in an ocean ecosystem. Mar. Ecol. Prog. Ser. 2008; 364: 15-29.

Wernberg T, Bennett S, Babcock RC, De Bettignies T, Cure K, Depczynksi M et al. Climate-driven regime shift of a temperate marine ecosystem. Science 2016; 353: 169-172.

Zuur AF, Tuck ID, Bailey N. Dynamic factor analysis to estimate common trends in fisheries time series. Can. J. Fish. Aquat. Sci. 2003; 60: 542–552.

Supporting Information

S1 Appendix: Standardization of time series from spatially resolved datasets.

S1 Table: Climate and biology time series included in the analyses

S2 Table: Summary information for the Bayesian DFA biology-covariate and biology only models (years 1981–2017).

S3 Table: Observations, predictions, and prediction errors for single species parameters in 2018.

S1 Figure: Climate and biology time series used in the study analyses.

S2 Figure: AR(1) coefficient on the southern/central California latent climate trend and support for a heavy-tailed deviations of the latent trend.

S3 Figure: The Student-t deviations degrees of freedom parameter (nu) in the southern/central California biology trend.

S4 Figure: A summary of the effect of the Cumulative Upwelling Transport Index (CUTI) on the individual single species parameter included in the DFA analyses

S5 Figure: A summary of the effect of the Isothermal Layer Depth (ILD) on the individual single species parameter included in the DFA analyses.

S6 Figure: A summary of the effect of the sea surface temperature on the individual single species parameter included in the DFA analyses

S7 Figure: Community variability in the southern California Current ecosystem (1981–2018).

S8 Figure: Forecasts and model estimates of the 'true' community state in the southern and central California Current in years 2009–2018.

S9 Figure: Fitted values for biology-covariate model including BEUTI (nitrate flux) as a covariate (1981–2017).

S10 Figure: Log coefficient of variation (CV) of 2018 predictions of individual species parameters plotted against the mean and log CV of loadings related to each species, and the mean and log CV of coefficients relating each species to BEUTI (nitrate flux).

Short Title: Tracking and forecasting community state

Tracking and forecasting community responses to climate perturbations in the California Current Ecosystem

Mary E. Hunsicker[1,†,*], Eric J. Ward[2,†], Michael A. Litzow[3], Sean C. Anderson[4], Chris J. Harvey[2], John C. Field[5], Jin Gao[6], Michael G. Jacox[7], Sharon Melin[8], Andrew R. Thompson[9], Pete Warzybok[10]

[1]Fish Ecology Division, Northwest Fisheries Science Center, National Marine Fisheries Service, National Oceanic and Atmospheric Administration, 2032 SE OSU Drive, Newport, OR 97365 US

[2]Conservation Biology Division, Northwest Fisheries Science Center, National Marine Fisheries Service, National Oceanic and Atmospheric Administration, Seattle, WA 98112 USA

[3]Alaska Fisheries Science Center, National Marine Fisheries Service, National Oceanic and Atmospheric Administration, Kodiak, AK 99615 USA

[4]Pacific Biological Station, Fisheries and Oceans Canada, Nanaimo, BC V9T 6N7 Canada

[5]Fisheries Ecology Division, Southwest Fisheries Science Center, National Marine Fisheries Service, National Oceanic and Atmospheric Administration, Santa Cruz, CA USA

[6]Centre for Fisheries Ecosystems Research, Memorial University of Newfoundland, St. John's, NL A1C 5R3 Canada

[7]Environmental Research Division, Southwest Fisheries Science Center, National Marine Fisheries Service, National Oceanic and Atmospheric Administration, Monterey, CA 93940 USA / Physical Sciences Laboratory, National Oceanic and Atmospheric Administration, Boulder, CO 80305 USA.

[8]Marine Mammal Laboratory, Alaska Fisheries Science Center, National Marine Fisheries Service, National Oceanic and Atmospheric Administration, Seattle, WA 98115 US

[9]Southwest Fisheries Science Center, National Marine Fisheries Service, National Oceanic and Atmospheric Administration, La Jolla, CA USA

[10]Point Blue Conservation Science, Petaluma, CA USA

*Corresponding author
Email: mary.hunsicker@noaa.gov

† These authors contributed equally to this work

Abstract

Ocean ecosystems are vulnerable to climate-driven perturbations, which are increasing in frequency and can have profound effects on marine social-ecological systems. Thus, there is an urgency to develop tools that can detect the response of ecosystem components to these perturbations as early as possible. We used Bayesian Dynamic Factor Analysis (DFA) to develop a community state indicator for the California Current Ecosystem (CCE) to track the system's response to climate perturbations, and to forecast future changes in community state. Our key objectives were to (1) summarize environmental and biological variability in the southern and central regions of the CCE during a recent and unprecedented marine heatwave in the northeast Pacific Ocean (2014–2016) and compare these patterns to past variability, (2) examine whether there is evidence of a shift in the community to a new state in response to the heatwave, (3) identify relationships between community variability and climate variables; and (4) test our ability to create one-year ahead forecasts of individual species responses and the broader community response based on ocean conditions. Our analysis detected a community response to the marine heatwave, although it did not exceed normal variability over the past six decades (1951-2017), and we did not find evidence of a shift to a new community state. We found that nitrate flux through the base of the mixed layer exhibited the strongest relationship with species and community-level responses. Furthermore, we demonstrated skill in creating forecasts of species responses and community state based on estimates of nitrate flux. Our indicator and forecasts of community state show promise as tools for informing ecosystem-based and climate-ready fisheries management in the CCE. Our modeling framework is also widely applicable to other ecosystems where scientists and managers are faced with the challenge of managing and protecting living marine resources in a rapidly changing climate.

Introduction

Climate perturbations can have strong impacts on ocean ecosystems that in turn affect social and economic components of human communities. These effects may be exacerbated when changes in ocean conditions are more extreme, such as during marine heatwaves. The increasing attention on these extreme events and their impacts (e.g., Hobday et al. 2018, Sen Gupta et al. 2020) has invigorated a push for tools that can track and detect as early as possible the response of marine communities to climate-driven perturbations. Early detection, and moreover, near-term forecasts of community shifts could help scientists, managers, and stakeholders better prepare for and respond to the potential consequences of such shifts.

Climate-driven shifts in community structure tend to involve rapid change across multiple populations that result in switches between contrasting community assemblages that may then persist for decades. A growing number of studies have documented community reorganizations in response to climate drivers (e.g., Beaugrand et al. 2008, 2015, Möllman and Diekmann 2012, Wernberg et al. 2016, Peabody et al. 2018). One of the best-known examples is the widespread northeast Pacific community reorganization that followed the 1976/1977 shift in the Pacific Decadal Oscillation (Benson and Trites 2002; Hare and Mantua 2000). The abrupt change from a cool to warm ocean regime had dramatic implications on ecosystem functioning and living marine resources (LMRs) throughout the region (Mantua et al. 1997, Anderson and Piatt 1999; Litzow and Ciannelli 2007, Peabody et al. 2018). Since then, northeast Pacific marine ecosystems have experienced several interannual or decadal perturbations that do not appear to have resulted in community-wide shifts of similar magnitude. However, between 2014 and 2016 these ecosystems experienced a marine heatwave that involved the warmest sea surface temperature (SST) and heat content anomalies that had ever been observed over large areas of

82 the North Pacific (Bond et al. 2015; Walsh et al. 2018). It was one of the most extreme
83 heatwaves globally in its combined magnitude, spatial scale, and duration (Hobday et al. 2018,
84 Sen Gupta et al. 2020), and the intense, persistent warming has been attributed to a combination
85 of natural and anthropogenic forcing (Jacox et al. 2018a; Laufkötter et al. 2020).
86 Several studies have documented myriad biological responses to this event. For example,
87 within the California Current Ecosystem (CCE), there were mass strandings of marine mammals
88 (Cavole et al. 2016), increased whale entanglements due to shifting prey sources (Santora et al.
89 2020), mass mortality events for marine seabirds (Cavole et al. 2016, Jones et al. 2018, Piatt et
90 al. 2020), a record-breaking domoic acid outbreak (McCabe et al. 2016), shifts in pelagic
91 macronekton and micronekton communities and species richness (Santora et al. 2017, Brodeur et
92 al. 2019, Nielsen et al. 2020), irruptions of previously rare fishes and invertebrates throughout
93 the California Current (Sakuma et al. 2016, Morgan et al. 2019, Sanford et al. 2019, Walker et al.
94 2020), and extraordinarily high recruitment of rockfishes (genus *Sebastes*; Schroeder et al. 2018,
95 Field et al. 2021) and northern anchovy (*Engraulis mordax*; Thompson et al. 2019). Yet, to date,
96 there have been few quantitative studies of how the marine heatwave impacted the broader CCE
97 community at multiple trophic levels, and therefore the importance of this extreme event for
98 community-wide patterns of variability, and the persistence of the community response, remains
99 largely unknown.
100 Indicators of community or ecosystem state are valuable tools for tracking climate-related
101 changes in ecosystem functioning and evaluating those changes within the context of past
102 climate perturbations (Harvey et al. 2020). Moreover, combining long-term monitoring surveys
103 and data with modeling frameworks that summarize information across taxa and life stages that
104 respond quickly to climate perturbations could provide early detection of an ecosystem shifting

105 into a novel state. Early detection of such shifts would benefit ecosystem-based and climate-
106 ready fisheries management strategies aimed at mitigating possible deleterious ecological and
107 socio-economic outcomes. There is also a pressing need for forecasts of future ecosystem states
108 to support forward-looking management of LMRs (Hobday et al. 2016, Tommasi et al. 2017,
109 Jacox et al. 2020), including assessments of risk. As climate models and forecasts of ocean
110 conditions continue to improve, the time is ripe for developing and testing methods that could
111 provide near-term forecasts of community state in relation to ocean conditions.

112 A challenge in summarizing ecosystem responses to perturbations is that time series used
113 to characterize the ecosystem often involve tens to hundreds of variables (species or climate
114 indices); there is often some degree of asynchrony among time series, and further, each is
115 corrupted by the presence of observation errors. Disentangling these sources of error and
116 separating the signal from the noise is statistically challenging. Traditionally, tools such as
117 Principal Components Analysis (PCA) or nonmetric multidimensional scaling have often been
118 used for identifying leading patterns of variability in multivariate datasets (e.g., Koslow et al.
119 2002, 2013); however, these approaches are ill-suited to the analysis of time series data that are
120 autocorrelated or non-stationary (Planque and Arneberg 2018). An alternative approach,
121 Dynamic Factor Analysis (DFA), is better suited for identifying shared trends that can be used as
122 a community state indicator. DFA is specifically designed for time series ordination, and avoids
123 many of the problems associated with other multi-variate approaches (Zuur et al. 2003). When
124 applied to a collection of multivariate time series, inference in DFA models focuses on
125 estimating a smaller number of temporal patterns ('trends') that best capture the variation
126 observed. The observed data are then treated as a mixture of these trends (Ward et al. 2019).
127 Ward et al. (2019) recently developed a Bayesian implementation of DFA that models shared

trends, detects "black swan" events (rare and difficult to predict events; Anderson et al. 2017), and estimates the probability of switches among contrasting system states. In the first application of this new method, Litzow et al. (2020a) examined shared trends of climate and biology time series in the Gulf of Alaska. Their study did not detect evidence for wholesale community reorganization during the recent northeast Pacific marine heatwave; however, their findings indicated potential for new patterns of ecosystem functioning with continued warming of ocean temperatures.

Here we build on this set of novel statistical tools to develop a model of the CCE state that can both track and forecast ecosystem changes in response to climate perturbations. Specifically, we expand the Bayesian implementation of DFA to test the community response to environmental variables within the modeling framework and to develop near-term forecasts of future community states. Using climate and biological data from the central and southern regions of the CCE, our goals were to: (1) summarize environmental and biological variability during 2014–2016 and compare these patterns to past variability; (2) assess the probability of observed departures from previous climate patterns and of switches to new states in community variability during the heatwave; (3) identify relationships, if any, between community variability and climate variables; and (4) test our ability to create one-year ahead simultaneous forecasts of species responses and the community state based on environmental information. While the focus of our study is the CCE, the approach applied here is widely applicable to the myriad marine ecosystems worldwide that are vulnerable to a rapidly changing climate.

Methods

Data

In our analysis, we used oceanographic time series from the southern (n=6) and central (n=6) regions of the CCE, derived from a data assimilative configuration of the Regional Ocean Modeling System (ROMS) with 0.1˚ (~10 km) horizontal resolution and 42 terrain-following vertical levels (Neveu et al. 2016; oceanmodeling.ucsc.edu). From the ROMS output, we generated monthly time series covering 1980-2018 for a suite of variables including sea surface temperature (SST), sea surface height (SSH), isothermal layer depth (ILD), Brunt-Väisälä frequency (BV), a coastal upwelling transport index (CUTI), and a biologically effective upwelling transport index (BEUTI). The ILD is similar to mixed layer depth and defines the depth where temperature deviates by 0.5˚C from the surface value. BV is a measure of water column stratification, averaged over the upper 200 m of the water column. CUTI and BEUTI are upwelling indices that quantify vertical transport and nitrate flux through the base of the mixed layer, respectively (Jacox et al. 2018b). The data were annually averaged (July-June) from the coast to 100 km offshore, with the exception of CUTI and BEUTI, which capture coastal upwelling within 75 km of shore. In the alongshore direction, we calculated averages for two regions with a division at Point Conception, California, separating the southern portion of the CCE (31–34.5˚N) from the central region (34.5-40.5˚N, Fig. 1). The annual averages were taken from July to June to capture the influence of the El Niño–Southern Oscillation (ENSO), which peaks in winter and is the dominant mode of interannual variability influencing the California Current. We developed models using ROMS output rather than empirical measurements because they provide full spatial and temporal coverage of surface and subsurface conditions, incorporate available observations, and will enable the use of ROMS forecasts to then forecast biological changes in the CCE. More details on the oceanographic time series can be found in S1 Table and S1 Figure.

Figure 1. Sampling locations of California Current Ecosystem biology included in the study analyses. Abundance data for pelagic juvenile groundfishes and invertebrates are collected on the Rockfish Recruitment and Ecosystem Assessment Survey (RREAS). Ichthyoplankton data are collected on the California Cooperative Oceanic Fisheries Investigations (CalCOFI) survey. Seabird reproductive success and California sea lion (*Zalophus californianus*) pup time series are collected on Southeast Farallon Island and San Miguel Island, respectively. See S1 Table and S1 Figure for detailed information on the individual time series.

The biology time series included in our analysis were selected based on three criteria: first, the measured variables would be expected to show rapid (0- to 1-year lag) responses to climate variability; second, the time series could be updated with no more than one year lag for processing time to increase the speed at which biological responses to perturbation could be detected; and third, the time series were at least 15 years long. The biology time series that met these criteria (n=38) included ichthyoplankton, pelagic young-of-the-year (juvenile fish), squid, and krill abundance; seabird productivity; and California sea lion pup body condition metrics (Fig. 1, S1 Table). These 38 time series were collected from four disparate ocean surveys, and span between 22 and 68 years. Datasets collected from surveys that included spatial attributes (e.g., ichthyoplankton and pelagic juvenile fish surveys) were first standardized using Generalized Additive Models to create a univariate time series for each species. While these datasets generally include spatial random sampling, the index standardization accounts for uneven distributions of effort (in space or time). Details on the standardization of individual datasets are included in S1 Appendix. In addition, the biology data were normalized with log

transformations where appropriate (all zeros were changed to NAs). For example, if the time series data were assumed to be lognormally distributed (e.g., weight/count data) or the coefficient of variation was > 1, the data were log transformed. All of the time series from an individual dataset (survey) were treated the same, i.e., logged or not. More details on the biology time series used in this study and the associated data sources and log transformations are summarized in S1 Table and S1 Figure.

Modeling

We describe the methods in detail below, but in summary our work flow was to (1) apply Bayesian DFA to climate and biology datasets separately and use model selection tools to identify the best supported model and number of shared trends, (2) apply 'black swan' and regime detection methods to detect extreme events and alternating community states, respectively, (3) identify whether the CCE community state was strongly correlated with the climate time series (compare performance of the biology models with/without environmental covariates), and (4) evaluate our skill at making predictions of community state and individual species variables.

Dynamic Factor Analysis

We used a Bayesian version of Dynamic Factor Analysis (DFA, Zuur et al. 2003, Ward et al. 2019) using the software Stan and R (R Core Team 2018) as implemented in the 'bayesdfa' package (Ward et al. 2020). DFA is a multivariate statistical tool somewhat analogous to Principal Components Analyses, but for time-series data (Holmes et al. 2018, https://cran.r-project.org/web/packages/MARSS/vignettes/UserGuide.pdf). For a collection of time series, the

number of estimated 'trends' is specified *a priori*, and DFA estimates these latent trends as independent random walks. In mathematical form, this is expressed as

$$\boldsymbol{x_t} = \boldsymbol{x_{t-1}} + \boldsymbol{w_{t-1}},$$

where $\boldsymbol{x_t}$ represents the value of latent (unobserved) trends at time *t*, and the process error deviations $\boldsymbol{w_{t-1}}$ are generally assumed to be white noise having arisen from a multivariate normal distribution (with an identity covariance matrix for identifiability). The latent trends are mapped to the observed data through an estimated loadings matrix $\mathbf{Z}$ and residual error $\boldsymbol{e}_t$,

$$\boldsymbol{y}_t = \mathbf{Z}\boldsymbol{x}_t + \boldsymbol{b} \cdot \boldsymbol{d}_t + \boldsymbol{e}_t,$$

where $\boldsymbol{y}_t$ is the vector of observed states at time *t*, and the residual error terms $\boldsymbol{e}_t$ are assumed to be drawn from a univariate or multivariate normal distribution. Though the covariance matrix of $\boldsymbol{w_t}$ is generally fixed (Zuur et al. 2003), the covariance matrix of $\boldsymbol{e}_t$ can be structured; variances may be shared or not across time series, and off diagonal elements may be estimated. The parameter vector $\mathbf{b}$ represents optional estimated coefficients relating covariates $\boldsymbol{d}_t$ to the observed response. In the context of our DFA modeling, we included climate variables as $\boldsymbol{d}_t$ in models where the biological observations were used as the response $\boldsymbol{y}_t$.

Because we implemented the DFA model in a Bayesian setting, we were able to extend this model to include additional features. First, to include extreme events, we relaxed the assumption about process errors $\boldsymbol{w_t}$ being drawn from a normal distribution and used a multivariate Student-t distribution instead (Anderson and Ward 2019). We also modified the process equation to consider an optional vector of AR(1) coefficients $\boldsymbol{\phi}$ on the latent trends. $\boldsymbol{x_t} = \boldsymbol{\phi x_{t-1}} + \boldsymbol{w_{t-1}}$ (Ward et al. 2019). A final modification of the conventional DFA model is that for some models, process variances can be estimated rather than fixed at 1 (maximum likelihood approaches generally use this constraint for identifiability). As implemented in Stan

(Stan Development Team 2016, Hoffman and Gelman 2014, Carpenter et al. 2017), we conducted estimation with three chains, with a warm-up of 2000 samples, followed by 2000 iterations. We used the split-chain potential scale reduction factor (Gelman and Rubin 1992, Gelman et al. 2013) to assess convergence (Rhat < 1.05). Code to replicate these analyses is deployed as an R package on CRAN ('bayesdfa', Ward et al. 2020) and our public Github repository, https://github.com/fate-ewi/bayesdfa.

We ran the DFA on climate datasets (1981–2017) and biological datasets (1951–2017) across the southern and central regions of the California Current combined. Running the analysis at this spatial scale allowed us to capture the broader community response to climate perturbations, compared to running models on each multivariate dataset independently (e.g., time series from a single survey). There are a number of ways to evaluate predictive accuracy of these models. Leave-One-Out Cross-Validation (LOO-CV), for example holds each observation out in turn and predictions are made from the remaining data. As our focus was on the temporal nature of the data and forecasting component, we implemented a variant of k-fold cross validation and treated individual years as unique 'folds'. Because our objectives involved evaluating these models for future predictions, we implemented the Leave-Future-Out Cross Validation Information Criterion (LFO-CV, Bürkner et al. 2020). We used this approach to identify data support for (1) the number of latent DFA trends (n = 1-3), (2) first-order autoregressive AR(1) coefficients on the trends ($\boldsymbol{\phi}$ estimated with a Normal(0,1) prior), (3) Student-t deviations (i.e., evidence of extreme events, using a prior on the MVT degrees of freedom parameter, ν, of $\nu \sim$ Gamma(2, 0.1)), and (4) a fixed versus estimated trend variance (using a prior on the standard deviation, σ_w, of $\sigma_w \sim \text{Normal}(0,1)$).

In addition, we used LFO-CV to identify the most appropriate error structure for the climate dataset—specifically whether the times series had equal (shared) or unequal (unique) observation errors. For the biology models, we assumed the observation errors were unique by dataset, and our estimates of survey variance supported this assumption.

For each model formulation, we applied the LFO-CV method by first fitting the model to all years of data prior to year *T* (i.e., training data) and then using the fitted model to predict the trend value in year *T* (i.e., test data). We repeated this process for 10 years, starting with 2017 as year *T* and working back to 2008, and then calculated the expected log predictive density (ELPD) across those time steps. The climate and biology models with the highest ELPD were deemed the best supported models. The LFO-CV is a preferred method for evaluating future predictive performance of Bayesian models because it properly accounts for time series structure, and unlike other Bayesian cross-validation methods, does not produce overly optimistic estimates (Bürkner et al. 2020).

Detection of extreme events and regime shifts

After identifying the best-supported DFA model for the climate and biological datasets, we conducted a post-hoc examination of outlier detection and regime shifts. For outlier detection of black swan events, we implemented a method similar to that described in Anderson et al. (2017) and applied it to the climate and biology time series. This approach relies on first differencing the posterior trend mean estimates of the climate and biology trends, $\boldsymbol{x}_t - \boldsymbol{x}_{t-1}$ and then applies a normal density function to identify year-over-year changes that were unlikely to have arisen from a normal distribution (given the process variance). Probabilities can then be assigned to the deviations in each year (e.g., 'there is a 1:1000 chance of observing a deviation

similar to that estimated in year *t*'). As described in Ward et al. (2019), the presence of regimes can also be estimated by applying hidden Markov models (HMM) to the estimated state indices from a DFA. We evaluated support for regimes and alternate states by using the posterior trend estimates from each model as input. The Bayesian Leave-One-Out cross validation Information Criterion (LOOIC, Vehtari et al. 2017) was used to identify the data support for the number of trends (n = 1–3).

Forecasting community state

While a wide variety of multivariate or univariate time series methods could be applied to our observed time series to generate forecasts, our objectives were to develop simultaneous estimates of both the community state(s) and the raw time series. We evaluated the ability of our DFA models to generate short-term (one year lead-time) forecasts of community state by first evaluating whether the performance of the biology DFA model was improved when climate time series were included as covariates in the model. If climate time series were found to better explain the variability in the biology time series, these relationships could potentially be used to forecast community trends. For our analysis, we ran the DFA on a subset of the biology data overlapping in time with the climate dataset, i.e., 1981–2017, to make out-of-sample predictions. We used the same LFO-CV procedure described above, with the same forecast period (2009–2017) to compare the biology models with and without a single climate covariate (see S2 Table for all model formulations). In this case, the model used biological and climate data from all preceding years and climate data from the year to be forecast. The six climate covariates from the southern region and the central region of the CCE (12 total) were tested in this analysis. Once the best-supported biology-covariate model was identified, we used that model to make

311 predictions of individual species parameters and the community state in 2018 using climate data
312 from that same year. We evaluated forecast skill based on the prediction errors of individual
313 species parameters and by comparing the forecasts for 2009–2018 to the 2009–2018 trend values
314 estimated from biology-covariate model that only included data prior to the forecast year.
315
316 **Results**
317 *Climate and biology trends*
318 The model with the highest predictive accuracy (ELPD) of the climate state in the southern and
319 central regions of the CCE was a one-trend DFA model (Model 1 in Table 1, Fig. 2a). This
320 model included unique observation variances across the six time series, support for heavy-tailed
321 deviations of the latent trend, an AR(1) coefficient on the trend (S1 Fig.), and an estimated trend
322 variance. All but one of the climate time series (central ILD) were associated with the single
323 trend, i.e., at least 90% of the loading posterior distributions associated with each time series
324 were above or below zero (Fig. 2b). The SST, SSH, and BV frequency (water column
325 stratification) time series from the southern and central regions of the CCE loaded positively on
326 this trend (Fig. 2b). The BEUTI and CUTI time series from both regions of the CCE and the ILD
327 time series from the central region loaded negatively on the trend (Fig. 2b). Overall, the trend
328 captured a well-documented cooling period in the CCE between 1980 and 2010 (e.g., Seo et al.
329 2012), as well as strong El Niño events (e.g., 1982–1983, 1997–1998, 2015–2016) and the 2014–
330 2016 marine heatwave. The trends and loadings indicate that these events were generally
331 associated with weaker upwelling, reduced mixed layer depth, low nutrient flux, and warm,
332 stratified waters (Fig. 2a, b).
333

Table 1. Summary information for climate and biology Bayesian DFA models, including whether process error was estimated, observation error variances (unequal or equal among time series, or unique to each survey), the number of model trends, expected log pointwise predictive densities (ELPD), and standard error of ELPD. Bold text highlights the models that show best support or highest predictive accuracy for the climate and biology data for the southern and central California Current ecosystem (i.e., highest ELPD). All climate and biology models include an AR(1) process and Student-t deviations.

Time series	Model	Process sigma	Variance index	Trends	ELPD	SE ELPD
Climate	1	Yes	unequal	1	**-10551.89**	759.44
	2	No	unequal	1	-10682.39	712.96
	3	Yes	equal	1	-16793.59	1732.54
	4	No	equal	1	-16881.03	1824.42
	5	No	unequal	2	-17441.01	1655.23
	6	Yes	unequal	2	-17818.86	1813.65
	7	Yes	unequal	3	-21571.65	1674.77
	8	No	unequal	3	-22882.99	1695.12
	9	No	equal	2	-23927.86	2694.72
	10	Yes	equal	2	-24536.19	2953.38
	11	Yes	equal	3	-38895.66	4024.93
	12	No	equal	3	-38920.87	4762.15
Biology	13	No	survey	1	**-2003.32**	95.76
	14	Yes	survey	1	**-2003.96**	88.88
	15	No	survey	2	-2155.52	76.05
	16	Yes	survey	2	-2198.79	78.86
	17	No	survey	3	-2334.55	118.31
	18	Yes	survey	3	-2335.10	112.70

Figure 2. Climate variability in southern and central California Current ecosystem: a) shared trend with 95% credible intervals (1981–2017), b) posterior distributions for loadings on all of the individual time series. Loadings with darker shading indicate time series loading most strongly on the climate trend. SST, sea surface temperature; SSH, sea surface height; ILD, isothermal layer depth; BV, Brunt-Väisälä frequency (stratification); CUTI, Coastal Upwelling

348 Transport Index; BEUTI, Biologically Effective Upwelling Transport Index. See S1 Table and
349 S1 Figure for climate times series details.
350
351 The climate state during the marine heatwave, as indicated by the DFA trend, was within
352 the bounds of previous observations. While there was support in the best model for heavy-tailed
353 deviations in the climate trend (i.e., Student-t deviations S1 Fig.), our post-hoc examination of
354 outliers detected a single extreme event in the climate state in mid-1998 to mid-1999
355 (threshold=0.001), when there was a shift from strong El Niño (1997–98) to strong La Niña
356 (1998–1999) conditions, and not around the time of the heatwave. Application of the Bayesian
357 HMM to the climate trend most supported the presence of two hidden states, reflecting the
358 probability of being in a state associated with warmer conditions versus one with cooler
359 conditions (LOOIC: one-state = 129.1, two-state = 9.4, three-state = 27.2, Fig. 3). The LOOIC
360 did not provide support for a shift to a third novel climate state in the southern and central
361 regions of the CCE during the marine heatwave, however there is a shift back to the previously
362 observed warm state during the marine heatwave.
363
364 **Figure 3.** Results of Hidden Markov Models (HMM) showing state probability for latent trends
365 in the climate (top) and biology (bottom) data sets. The best model for both data sets invoked
366 two states, and the median probability (and 95% credible intervals) of being in one state versus
367 the other is shown. The top figure reflects the probability of being in the state associated with
368 warmer conditions versus one with cold conditions, and bottom figure indicates that ecosystem
369 did not shift into a new state following the marine heatwave.
370

371 The best model for community variability among our biological time series was also a
372 one trend model (Model 13 in Table 1, Fig. 4a). The model formulation was similar to the best
373 climate model, except the observation variances were unique by dataset (survey) and not
374 individual time series. We note that the top two models (Model 13 and 14) showed similar
375 predictive accuracy (Δ ELPD < 1) and only differed with respect to whether the process variance
376 was fixed at 1 or estimated. Here we only show results for the model with a fixed process
377 variance. The biology showed strong coherence in community signal; a majority of the time
378 series (31 of 38) loaded strongly (probability > 0.9) on the single trend and most of them
379 demonstrated loadings in the same direction (Fig. 4b). The magnitude and direction of the
380 estimated loadings were consistent with the observed high relative abundance of most juvenile
381 groundfishes (rockfish, flatfish), squid, krill, and some ichthyoplankton species increased during
382 the marine heatwave, and suggest that the reproductive success of some seabird species was
383 higher around the time of the heatwave as well. The few time series loading in the other direction
384 on the trend indicated a reduction in sea lion pup growth rate and lower abundances of
385 juvenile/adult Pacific sardine *Sardinops sagax* and some ichthyoplankton species (e.g., larval
386 northern anchovy and Pacific hake *Merluccius productus*) associated with the heatwave.
387
388 **Figure 4.** Community variability in the southern California Current ecosystem: a) shared trend
389 with 95% credible intervals (1951–2018), b) posterior distributions for loadings on individual
390 time series (only time series with ≥ 90% of the loading distributions above or below zero are
391 shown). Loadings with darker shading indicate time series loading most strongly on the biology
392 trend. Cal. = California, Juv. = juvenile fish stage, Juv./adult = juvenile and adult fish stages
393 combined, all other fish are larval fish. See S1 Table and S1 Figure for times series details.

The estimated trend from this biology DFA model demonstrates a potential shift in community state in the mid-1960s, although there is considerable uncertainty around the trend during this early portion of the time series, likely due to the limited number of observations (ichthyoplankton only) pre-dating the 1970s (Fig. 4a, S1 Fig.). Similarly, the limited number of biological time series and missing sampling years in the late 1960s and 1970s, and the lack of climate outputs from ROMS prior to 1980, make it difficult to detect a documented transition that happened in the mid-1970s (S1 Fig., see discussion). The community state appears to be relatively stable from the late 1970s through the early 2000s, and the trend reached a peak around 2013–2015. Evidence of a community shift early in the time series is supported by our regime detection analysis, which demonstrated that a two-state model best described the latent trend (LOOIC: one-state = 216.4, two-state = 11.8, three-state = 41.8, Fig. 3). This shift coincides with a strong increase in the abundance of a few species during that period, including eared blacksmelt (*Lipolagus ochotensis*), slender blacksmelt (*Bathylagus pacificus*), northern lampfish (*Stenobrachius leucopsarus*), as well as a rise in northern anchovy (*Engraulis mordax*) abundance prior to the shift (S1 Fig.). Our analysis does not document a shift to a novel community state in response to the recent marine heatwave.

While this model provided slight support for heavy-tailed Student-t deviations in the latent trend (S2 Fig.), we did not detect any black swan events in the community state. We note that the community response to two strong El Nino events (1982–1983 and 1997–1998) and to unusually low productivity conditions (2005) in the central CCE appear similar in magnitude and duration to the response to the 2014-2016 marine heatwave, although the directions of the responses were opposite (Fig. 4a). Our regime detection analysis also captured the change in the

central CCE community in the mid to late 2000s (Fig. 3), which may be associated with the large changes in the reproductive success of multiple seabirds (e.g., Cassin's auklet, common murre, Brandt's cormorant) and in sea lion pup births around that time (S1 Fig). These taxa may have been impacted by changes in the abundance or availability of important prey items resulting from unproductive ocean conditions in the central CCE in 2005 and the below normal SSTs associated with the 2007-2008 La Nina Event (McClatchie et al. 2008, 2009, Bjorkstedt et al. 2010).

Forecast of community state

In comparing models of the biological response with and without climate covariates, we found that several biology models with climate predictors outperformed the biology models that did not include covariates (S2 Table). The climate covariate resulting in the best future predictions of community state was BEUTI (central region), followed by CUTI (central region) (Table 2, see S2 Table for all models). The coefficients linking BEUTI to observed time series (**B** matrix) indicate strong, positive relationships between nitrate flux and the reproductive success of seabirds and the abundance of krill in the central California Current (Fig. 5). They also indicate strong, negative relationships between nitrate flux and the abundance of juvenile/adult Pacific sardine and larval northern anchovy (Fig. 5). The remaining biology-BEUTI relationships were moderate (e.g., ichthyoplankton, market squid *Doryteuthis opalescens*) to weak (e.g., rockfish spp., Fig. 5). The biology-CUTI model was similar to the biology-BEUTI model with respect to model structure and estimated species loadings. The estimated coefficients in the CUTI model also show a similar pattern to those in the biology-BEUTI model (S5 Fig.). The remaining covariate models only showed weak climate-biology relationships (e.g., S5-S6 Fig.).

Table 2. Summary information for the top biology-covariate Bayesian DFA models for each covariate and the top two biology only models (years 1981-2017). The table indicates whether process error was estimated ('Yes') or fixed ('No'), the number of model trends, expected log pointwise predictive densities (ELPD), standard error of ELPD, the environmental covariate included in the model, and the region in the California Current over which the covariate was aggregated. All models had an AR(1) coefficient on the trend and Student-t deviations. Model 1 was deemed the best model based on its highest predictive accuracy (highest ELPD value) compared to all other models. BEUTI = Biologically Effective Upwelling Transport Index; BV = Brunt-Väisälä frequency; CUTI = Coastal Upwelling Transport Index; ILD = Isothermal Layer Depth; SST = Sea Surface Temperature; SSH = Sea Surface Height. See S2 table for the full suite of model comparisons.

Model	Process sigma	Trends	ELPD	SE ELPD	Covariate	Region
1	**No**	**1**	**-1878.71**	**71.52**	**BEUTI**	**central**
2	No	1	-1905.27	81.98	CUTI	central
3	No	1	-1914.62	83.22	ILD	south
4	No	1	-1927.33	88.26	SST	south
5	No	1	-1928.03	88.39	BV	south
6	No	1	-1946.75	86.33	SSH	south
7	No	1	-1951.44	73.59	None	-
8	Yes	1	-2038.71	91.44	None	-

Figure 5. A summary of the effect of the Biologically Effective Upwelling Transport Index (BEUTI), a measure of nitrate flux through the base of the mixed layer, on the single species parameters. Cal. = California, Juv. = juvenile fish stage, Juv./adult = juvenile and adult fish stages combined, all other fish are larval fish. Blue error bars reflect 95% credible intervals. Figures S4-S6 show effects of other environment covariates on the biological variables.

Given that the biology-BEUTI model was the best supported model over the null model (a model without covariates), we were interested in evaluating the ability of this covariate model to forecast the community state. Comparisons between the community state (out-of-sample estimates) and the community state forecasts indicate that we had skill in forecasting community state one year in advance (Fig. 6, S7 Fig., S8 Fig.). Forecasts of the community trend values for nine additional years (2009–2017, S8 Fig.) also indicate that we had some skill for many of the years tested. There are wide confidence intervals around the forecasts; however, given our methodology we can expect that the credible intervals around the trend forecast will be larger than the historical credible intervals (Fig. 6). Forecasts have more uncertainty than historical values because the variance of a random walk increases linearly with time (Holmes 2004; Ward et al. 2014). Furthermore, our credible intervals are increased because we are additionally (1) propagating full parameter uncertainty across the MCMC draws projecting it, and (2) using a Student-t distribution, which has heavy tails and therefore makes the uncertainty intervals wider than if we used normal distribution.

Figure 6. Community variability and forecast of the community state in the southern California Current. The shared biology trend (blue line, with 95% credible intervals) derived from biology-BEUTI model fit to subset of data (1981–2018) is shown along with the trend forecast for 2018 (circle, with 95% credible intervals). See S7 Fig. for model loadings.

Overall, the model forecast skill of individual species parameters was moderate to high for half of the species included in the biology-BEUTI model (S3 Table, S9 Fig.). It is important

to emphasize that the source of variability in predictions for each of the original time series is a mixture of the magnitude and uncertainty around the trends and loadings ($\boldsymbol{x}_t$, $\mathbf{Z}$), and the magnitude and uncertainty in the estimated covariates ($\boldsymbol{b}$). On the one hand, the time series associated with the highest predictive skill (i.e., lowest prediction errors) included seabird reproductive success (Common murre *Uria aalge*, Cassin's auklet *Ptychoramphus aleuticus*) and the abundance of juvenile Pacific sanddab *Citharichthys sordidus*, juvenile halfbanded rockfish *Sebastes semicinctus*, market squid, and several ichthyoplankton species (S3 Table, S9 Fig.). On the other hand, forecast skill was lowest (i.e., highest prediction errors) for the abundance of some juvenile rockfishes (chilipepper *Sebastes goodei* and widow rockfish *Sebastes entomelas*) and larval fishes (northern anchovy, mesopelagics), which is likely attributed to a lag or mismatch in the timing of the climate-biology relationships. These patterns in forecast skill are similar to those based on the biology-CUTI, -SST, and -ILD models (S3 Table). Lastly, the uncertainty around model predictions of species parameters appears to be driven more by the precision of the model coefficients than by the loadings on the community trend (e.g., S10 Fig.).

Discussion

We applied a novel set of statistical tools to data from the southern and central regions of the CCE to document the community response to climate perturbations over the past six decades and to create near-term forecasts of community state. Our analysis detected a community response to the 2014-2016 northeast Pacific marine heatwave; however, it did not exceed normal variability within the study timeframe or result in a shift to a novel community state, based on the biological time series investigated here. We identified relationships between community state and multiple climate variables, with nitrate flux through the base of the mixed layer having the strongest

505 correspondence with individual species time series and the shared trend in community
506 variability. Moreover, we demonstrated skill in creating simultaneous one-year lead time
507 forecasts of species responses and community state.
508 There have been several studies and anecdotal evidence of unexpected biological
509 responses to the 2014–2016 northeast Pacific marine heatwave. Based on the biological time
510 series included in our analysis, the broader CCE community demonstrated a response to the
511 marine heatwave, i.e. the biology trend is higher over those years than in previous years.
512 However, our results do not demonstrate a widespread community reorganization beyond the
513 archetypal community structure of this recognizably dynamic ecosystem within the southern and
514 central CCE in response to this event. Instead, the mean values for the shared trend in the
515 biology time series, as well as for the shared climate trend, were within the range of previous
516 observations. An unusual aspect of the 2014–2016 events, relative to past warming associated
517 with El Niño or other low-productivity warm periods, was the very high abundance of young-of-
518 year rockfish and anchovy (Santora et al. 2017, Thompson et al. 2019, Schroeder et al. 2019),
519 which differed from most past warm events in which the abundance of these taxa was greatly
520 reduced. There were many species present during the marine heatwave that are not typically
521 observed in sampling or associated with the CCE, but those exceptional presences and high
522 abundances of warm species did not result in a persistent signal among the species for which we
523 have time series contributing to the DFAs. While our study did not detect a shift in community
524 state in the southern and central CCE during the 2014–2016 heatwave, we did detect a shift in
525 the 1960s. The 1960s shift was likely due to a regime shift previously detected in the southern
526 California ichthyoplankton community (Peabody et al. 2018); the southern California
527 ichthyoplankton time series are the only data used in our analysis that pre-date the 1970s.

Peabody et al. (2008) identified several species that caused the 1960s shift and their study included a much broader suite of ichthyoplankton species than our study which limits our ability to evaluate whether the species driving the shifts are consistent among studies**.** Previous studies also documented a shift in response to the 1977/1978 PDO shift (e.g., McGowan et al. 2003, Peabody et al. 2018) while our analyses did not. Our estimated biology trend is consistent with the evidence of this regime shift, however, only ichthyoplankton time series are available prior to the 1970s and there are gaps in the ichthyoplankton data between the late 1960s through the 1970s (CalCOFI only sampled every third year during this time). The trend estimate therefore has higher uncertainty during this period than elsewhere in the time series. This likely limits any detection of a regime shift in the mid to late 1970s. In a recent study, Litzow et al. (2020a) applied Bayesian DFA to 11 climate time series and 48 biology time series in the Gulf of Alaska (GOA). While their study revealed markedly elevated values in a shared climate trend between 2014–2019, it did not provide evidence of a shift to a novel mean state in shared trends of ecosystem variability during the extreme warming event. Their analysis did, however, capture the rapid community change in the GOA following the 1970's PDO shift in the northeast Pacific Ocean. We note that our study, as well as Litzow et al. (2020a), are based on time series that only extend a few years beyond the heatwave. As additional years of data become available, the CCE and GOA Bayesian DFA models could reveal different outcomes. However, this is unlikely given that the taxa and life stages used in both studies are known to respond quickly to changes in ocean conditions, i.e., within less than one year, and given our assumption that the surveys are consistently sampling at the right time and location to fully characterize the short-term response.

A compelling outcome of our analysis and the similar analysis of Alaskan species by Litzow et al. (2020a) is that neither detected state changes in North Pacific communities

following the massive 2014-2016 marine heatwave, despite the extremely anomalous physical conditions throughout most of the basin and a litany of concurrent biological, ecological, social and economic effects (see Introduction). An important characteristic of both studies is the temporal scale of community analysis (1972-2017 for the GOA and 1951-2017 for the CCE). This long temporal scale provides an important context for comparing contemporary change with the magnitude of historical community shifts. In addition, the Bayesian DFA accounts for uncertainty in the shared trends in a way that prevents premature detection of wholesale ecosystem shifts. We note that Suryan et al. (2021), fitted a single-trend, non-Bayesian DFA model to a larger set of GOA biological time series (n = 187) over a shorter time span (2010-2018) and found evidence of a well-resolved shift that implied different community states during 2010-2014 and 2015-2018. The different conclusions of Suryan et al. (2021) and Litzow et al. (2020a) studies speak to an inherent tension in retrospective analyses of community change. Limited time series availability means that analyses can be taxonomically and functionally broad (e.g., Suryan et al. 2021), or temporally extensive (e.g., Litzow et al. 2020a), but not both. Each approach has advantages, but direct comparison between the two is difficult. Given the impacts of the 2014-2016 event, and that long-term warming combined with marine heatwaves will push the CCE into novel climate states, we must consider ecological mechanisms that might explain why these communities were apparently resilient to the marine heatwave, along with revisiting methodological details that could further clarify our results.

The CCE shared biology trend and loadings captured unexpected patterns in the community response to regional climate perturbations. The biology time series included in this study showed strong coherence in community signal in response to regional climate perturbations across multiple trophic levels, life-history strategies, and datasets. Most of the

biological time series loaded in the same direction on the shared trend, with only a few time series showing the opposite pattern. In addition, several species that are typically associated with cooler ocean conditions show increased relative abundances during the marine heatwave. For example, past studies have shown that high abundances of pelagic juvenile rockfish and groundfish, squid, and krill are associated with more southward transport in the California Current, and more subarctic source waters, with abundance far lower in years with more subtropical waters, which are often associated with El Niño and anomalous warm events (Ralston et al. 2015, Schroeder et al. 2019). Our analysis captured this documented pattern, showing a reduced abundance of these species that have been associated with subarctic source waters and strong equatorward flow in the California Current during two of the strongest El Nino events on record (1982–1983, 1997–1998) and unusually low productivity conditions (2005–2006, Peterson et al. 2006). Our analysis also captured the unexpected increase in abundance of these taxa in 2014–2016 despite the anomalously warm ocean conditions at that time. This may be partially explained by the observation that subsurface waters were more subarctic, rather than subtropical in origin (Schroeder et al. 2019) and that there was some strong upwelling during the marine heatwave, particularly in spring 2015 (Peterson et al. 2015, Ryan et al. 2017). The reduced production of juvenile/adult Pacific sardine and increase in juvenile northern anchovy between 2014 and 2016 shown here and elsewhere (Thompson et al. 2019) were consistent with a history of observations indicating that these species tend to respond asynchronously to ocean conditions (MacCall 1996, Schwartzlose et al. 1999, Chavez et al. 2003, Deyle et al. 2013, Sydeman et al. 2020). However, the responses were of opposite sign from past observations of increases in sardines and decreases in anchovy under warm conditions (Chavez et al. 2003). The DFA trends and loadings indicate a negative response of sea lion pup growth and weight to the

2014–2016 marine heatwave, which also aligns with past work showing that reduced prey availability for nursing mother sea lions is unfavorable for sea lion pups (McClatchie et al. 2016). Notably, sea lion pup condition covaried with abundance of anchovy and sardine, which provide quality prey to sustain lactation. Pup condition also improved at the tail end of the marine heatwave when, despite the warm water, anchovy abundance increased dramatically and by 2017 all metrics of pup condition were above average (Thompson et al. 2019). In addition, the trends and loadings suggest that the reproductive success of some seabirds in the central region of the CCE was not diminished by the heatwave, although recent studies have documented the severe impact of the heatwave on seabird productivity in regions to the north (Piatt et al. 2020). Our analysis is not able to capture the irruptions of fishes and invertebrates that are rare in long-term CCE time series. Many sporadically occurring taxa such as pelagic red crabs (*Pleuroncodes planipes*), which are absent from California waters in most years but abundant infrequently in warm years with anomalous transport from the south, are not well suited to include as time series due to large number of zero observations in the survey data.

Incorporating climate information in DFA models of CCE biology indicated that models with a climate covariate performed better than models without one. The model results suggest that nitrate flux into the surface mixed layer (BEUTI) was the best covariate for individual species in addition to the shared trend in the southern and central CCE over the past three decades. Nitrate flux had a strong positive effect on the abundance of krill and some larval fishes and on the reproductive success of seabirds, and a moderate positive effect on some pelagic juvenile fishes, squid, and sea lion pup births. Stronger upwelling magnitude (CUTI), which is correlated with nitrate flux, was the second-best predictor of community variability and had a positive albeit weaker effect on the same suite of species (S4 Fig.). These findings are consistent

620 with mechanistic understanding as upwelling increases the supply of nutrients from deep to
621 shallow waters and enhances the productivity at the lower trophic levels that affect foraging
622 conditions for higher trophic level species in coastal habitats. For example, past work has shown
623 that rockfish abundance is positively associated with upwelling strength (Ralston et al. 2013),
624 and seabird productivity has been shown to increase when ocean conditions support high primary
625 production and higher trophic level prey (e.g. Wells et al. 2008). Rockfish production is also
626 higher when subsurface source waters in the California Current are more subarctic rather than
627 subtropical, which may explain the negative effect of isothermal layer depth (ILD) and
628 temperature on some rockfish species (S5 Fig., S6 Fig.). More subtropical source waters and
629 surface warming tend to be associated with deeper isopycnals, higher stratification, and
630 shallower ILD (Schroeder et al. 2019, Bograd et al. 2019). Nitrate flux (BEUTI) had a strong
631 negative correlation with juvenile/adult Pacific sardine and larval northern anchovy and
632 upwelling strength (CUTI) did as well. The relative abundance of Pacific sardine in coastal
633 waters off of Central California has been shown to be lower during periods of strong upwelling
634 (Santora et al. 2014, Ralston et al. 2015). This trend may reflect a change in the production of
635 Pacific sardine or a shift in their relative distribution. In addition, a negative relationship between
636 upwelling and nitrate flux and sardine recruitment can generally be explained by the transfer of
637 fish larvae to offshore areas where they have low chance of survival during periods of strong
638 equatorward flow and upwelling (Bailey and Francis 1985, Nieto et al. 2014), although our
639 understanding of the mechanisms driving anchovy population dynamics is limited (Sydeman et
640 al. 2020). We acknowledge that climate drivers often act in concert to influence community
641 variability, and here we are evaluating the effects of the climate variables one at a time. An
642 important next step of this work will be to examine whether including multiple climate

643 covariates in the CCE biology model further improves the forecast skill of the model and our
644 community state indicator. However, the individual climate variables are collinear and share
645 information, which affects our ability to makes inference on the covariates. Furthermore, our
646 study is an attempt to synthesize a broader suite of community indicators and their response to
647 climate perturbations and therefore should not be interpreted as replacing or simplifying more
648 detailed investigations into the drivers and mechanistic understanding of the indicators included
649 here.

650 Our approach for creating simultaneous predictions of species responses and shared
651 ecosystem variability to ocean conditions shows promise for developing near-term forecasts of
652 community state. Our forecasts are based on ocean model data derived from the CCE ROMS,
653 which have been applied in several recent studies to examine how oceanographic processes
654 affect fish recruitment variability (Tolimieri et al. 2018, Haltuch et al. 2020) and productivity
655 (Siegelman-Charbit et al. 2016), species habitat suitability (Abrahms et al. 2018, Cimino et al.
656 2020), and species spatial distributions (Muhling et al. 2019, 2020). The CCE ROMS also
657 supports nowcasts of species distributions based on observed ocean conditions that can help
658 resource managers and users manage risks associated with fisheries bycatch and ship-strike
659 (Hazen et al. 2017, 2018, Welch et al. 2019). Moreover, multiple efforts are underway in the
660 CCE and other coastal systems to develop short-term forecasts (1–24 months) of ocean
661 conditions for uptake by scientists, managers, and other end-users (Siedlecki et al. 2016, Kaplan
662 et al. 2016, Jacox et al. 2020, Malick et al. 2020). Here, we were able to create forecasts of
663 community state and several individual species parameters one year in advance based on
664 observations of a single climate variable (nitrate flux). The lead-time of such a forecast could be
665 extended further by using forecasts of ocean conditions rather than observed conditions, and

ocean temperatures in the CCE can be skillfully forecast months to a year in advance, with particularly high skill in the late winter and spring (Jacox et al. 2019). As mentioned above, future extensions of our work will evaluate whether a combination of climate variables as well as time lags might improve our forecasting skill.

In the CCE, nonstationary relationships are an important consideration for producing reliable ecological forecasts in this ecosystem. While the year-to-year variability in the estimated trend did appear to be stationary for our community models (Fig. 4, 6), the autocorrelation appeared to be nonstationary with the lag-1 autocorrelation between 2000–present being significantly higher (0.82) than over the years 1981–2000 (0.23). In addition to nonstationary variance parameters, future analyses may also consider nonstationary relationships in the covariate relationships, or potential interactions between covariates. A growing number of retrospective analyses have revealed nonstationary relationships among climate and individual species or community-level variables (Puerta et al. 2019, Litzow et al. 2018, 2019, 2020 a,b,c). In the northeast Pacific Ocean, these studies have been mostly focused on Alaskan ecosystems, which have long time series that support robust statistical analysis of nonstationarity in climate and biological systems. The best-documented instance of nonstationary relationships among climate and biology time series in the North Pacific centers on a climate shift in the late 1980s (Litzow et al. 2020b). Decades of observational data on either side of that event allow for statistically robust tests for nonstationarity that are not yet available for post-2014–2016 conditions. The problem of having few years of available data is an inescapable limitation for evaluating the possibility that nonstationary relationships might accompany emerging, novel climate conditions. Similarly, the considerable historical and paleoceanographic evidence for low frequency variability in the productivity of many key marine populations, particularly coastal

689 pelagic species such as Pacific sardine and northern anchovy, also complicates the challenges
690 associated with detecting nonstationarity with data of a limited temporal duration (Baumgartner
691 et al. 1992, MacCall 1996, Field et al. 2009), although such patterns may lead to greater risk of
692 "detecting" nonstationarity when in fact it may not exist (Cohn and Lins 2005, Milly et al. 2015).
693 However, early indications from Alaska suggest the possibility that long-standing relationships
694 between leading climate modes and individual climate and biology time series may have
695 changed following 2014 (Litzow et al. 2020c).

696 Using DFA to forecast attributes of community structure in the CCE allows us to create
697 simultaneous forecasts of trends, or 'ecosystem state', and raw time series. This approach could
698 also be applied individually to each dataset in our analysis to generate taxa-specific indicators
699 (e.g., seabird productivity, juvenile fish abundance), though forecasts would be expected to differ
700 from those with the entire CCE data. Similarly, if ecosystem states were not a focus of inference,
701 alternative forecast models could be applied (e.g., ARIMA or non-parametric models, Ward et al.
702 2014). Forecasts for individual time series from the DFA models used here can be seen as a
703 mixture of the AR forecast on the estimated trends (Fig. 6), and linear effects of forecasted
704 climate variables on each time series (Fig. 5). Species that have strong associations or loadings
705 on the trend and estimated climate effects that are large in magnitude (e.g., market squid, Pacific
706 sanddabs, shortbelly rockfish *Sebastes jordani*) are expected to have the most accurate
707 predictions, while those species with weak loadings and weaker effects of climate variables (e.g.,
708 California smoothtongue (*Leuroglossus stilbius*) are expected to have worse forecast
709 performance.

710 Our approach for developing a community state indicator to track and predict the
711 response of marine ecosystems to climate perturbations has the potential to support ecosystem-

based and climate-ready management in multiple ways. Garnering knowledge of community state and the potential for large shifts in ecosystem structure in response to intense and novel climate perturbations can help inform better, more rapid management decisions for mitigating ecological and socioeconomic impacts. The combination of long-term monitoring surveys and data with the modeling framework we advance here can also help scientists identify or refine key variables of ecosystem change that are summarized for ecosystem assessments in support of decision-making (Harvey et al. 2020). For example, it might be prudent to emphasize ecological time series that load strongest on ecosystem state trends and demonstrate strong, predictable relationships with climate variables (or other covariates of interest) over time series with weaker loadings on shared trends of community variability or have low forecast skill with environmental variables. Furthermore, our approach can provide valuable ecosystem information for scientific, management and coastal communities during times when researchers cannot sample the biology in marine ecosystems. This added value became acutely apparent in 2020 when myriad ocean surveys were cancelled or limited in spatiotemporal scope due to safety restrictions associated with the COVID-19 pandemic. Finally, our approach provides a quantitative way to help managers discern short-term periods of unusual community dynamics and/or high variability—such as the 2014-2016 marine heatwave—from state shifts that represent more enduring transitions into new regimes of ecosystem structure or productivity. Given that global climate change is expected to amplify ocean change, approaches like the one applied here will become increasingly valuable for marine resource management and conservation.

Acknowledgements

We thank those who have spent countless hours planning field surveys and collecting data for the invaluable time series used in our study. We thank the U.S. Fish and Wildlife Service for granting permission and providing resources to conduct research on the Farallon Islands National Wildlife Refuge. Funders for Point Blue's Farallon Research Program include the Bently Foundation, Elinor Patterson Baker Trust, Bernice Barbour Foundation, Frank A. Campini Foundation, Grand Foundation, Kimball Foundation, Marisla Foundation, Giles W. and Elise G. Mead Foundation, Moore Family Foundation, RHE Charitable Foundation, Volgenau Foundation, and numerous individual donors. We thank B. Feist for creating the map of the sampling areas (Figure 1). We thank N. Tolimieri and T.L. Rogers for their helpful comments that improved this manuscript. Funding for this project came from NOAA's Fisheries and the Environment (FATE) program (project 16-01) and NOAA's California Current Integrated Ecosystem Assessment program.

References

Abrahms B, Welch H, Brodie S, Jacox MG, Becker EA, Bograd SJ et al. Dynamic ensemble models to predict distributions and anthropogenic risk exposure for highly mobile species. Divers. Distrib. 2019; 25: 1182-1193. doi: 10.1111/ddi.12940.

Anderson SC, Ward EJ. Black swans in space: modelling spatiotemporal processes with extremes. Ecology 2019; 100: e02403. doi:10.1002/ecy.2403.

Anderson SC, Branch TA, Cooper AB, Dulvy NK. Black-swan events in animal populations. Proc. Natl. Acad. Sci. U.S.A. 2017; 114: 3252–3257.

Anderson PJ. Piatt JF. 1999. Community reorganization in the Gulf of Alaska following ocean climate regime shift. Mar. Ecol. Prog. Ser. 1999; 189: 117-123.

Bailey KM, Francis RC. Recruitment of Pacific Whiting, Merluccius productus, and the ocean environment. Mar. Fish. Rev. 1985; 47: 8-11.

Baumgartner TR, Soutar A, Ferreira-Bartrina V. Reconstructions of the history of Pacific sardine and northern anchovy populations over the past two millennia from sediments of the Santa Barbara Basin, California. CalCOFI Rep. 1992; 33: 24-40.

Beaugrand G, Edwards M, Brander K, Luczak C, Ibanez F. Causes and projections of abrupt climate-driven ecosystem shifts in the North Atlantic. Ecol. Lett. 2008; 11: 1157–1168.

Beaugrand G, Conversi A, Chiba S, Edwards M, Fonda-Umani S, Greene C et al. Synchronous marine pelagic regime shifts int he Northern Hemisphere. Phil. Trans. R. Soc. 2016; 370: 20130272. doi: 10.1098/rstb.2013.0272.

Benson AJ, Trites AW. Ecological effects of regime shifts in the Bering Sea and eastern North Pacific Ocean. Fish Fish. 2002; 3: 95–113.

Bjorkstedt EP, Goericke R, McClatchie S, Weber E, Watson W, Lo N et al. State of the California current 2009-2010: Regional variation persists through transition from the la Niña to el Niño (and back?). CalCOFI Rep. 2010; 51.

Bograd S, Schroeder ID, Jacox MG. 2019. A water mass history of the Southern California current system. Geophys. Res. Lett. 2019; 46: 6690-6698.

Bond NA, Cronin MF, Freeland H, Mantua N. Causes and impacts of the 2014 warm anomaly in the NE Pacific. Geophys. Res. Lett. 2015; 42, 3414–3420. doi: 10.1002/2015GL063306.

Bürkner P-C, Gabry J, Vehtari A. 2020. Approximate leave-future-out cross-validation for Bayesian time series models. J. Stat Comput. Simul. 2020; 90: 2499-2523.

Brodeur RD, Auth TD, Phillips AJ. Major shifts in pelagic micronekton and zooplankton community structure in an upwelling ecosystem related to an unprecedented marine

heatwave. Front. Mar. Sci. 2019. doi: 10.3389/fmars.2019.00212.

Carpenter B, Gelman A, Hoffman MD, Lee D, Goodrich B, Betancourt M et al. Stan: A Probabilistic Programming Language. J. Stat. Softw. 2017. doi: 0.18637/jss.v076.i01.

Cavole LM, Demko AM, Diner RE, Giddings A, Koester I, Pagniello CM et al. Biological impacts of the 2013–2015 warm-water anomaly in the Northeast Pacific: winners, losers, and the future. Oceanography 2016; 29, 273–285.

Chavez FP, Ryan J, Lluch SE, Niquen MC. From Anchovies to Sardines and Back: Multidecadal change in the Pacific Ocean. Science 2003; 299: 217-221.

Cimino MA, Santora JA, Schroeder I, Sydeman W, Jacox MG, Hazen EL, Bograd SJ. Essential krill species habitat resolved by seasonal upwelling and ocean circulation models within the large marine ecosystem of the California Current System. Ecography 2003; 43, 1-15. doi: 10.1111/ecog.05204.

Cohn TA, Lins, HF. Nature's style: Naturally trendy. Geophys. Res. Lett. 2005. doi: 10.1029/2005GL024476

Deyle ER, Fogarty M, Hsieh C-h, Kaufman L, MacCall AD, Munch SB et al. Predicting climate effects on Pacific sardine. Proc Natl Acad Sci USA 2013; 110: 6430-6435.

Field DB, Baumgartner TR, Ferreira V, Gutierrez D, Lozano-Montes H, Salvatteci R, Soutar A. Variability from scales in marine sediments and other historical records. In: Checkley DM, Alheit J, Oozeki Y, editors. Climate change and small pelagic fish. Cambridge: Cambridge University Press; 2009. pp. 45-63.

Field JC, Miller RA, Santora JA, Tolimieri N, Haltuch MA, Brodeur RD et al. Spatiotemporal patterns of variability in the abundance and distribution of winter-spawned pelagic juvenile rockfish in the California Current. PloS one 2021; 16: e0251638.

803 Gelman A, Carlin JB. Stern HS, Dunson DB, Vehtari A, Rubin DB. Bayesian Data Analysis. 3rd
804 ed. CRC Press; 2013.
805 Gelman A, Rubin DB. Inference from Iterative Simulation Using Multiple Sequences. Statist.
806 Sci. 1992; 7: 457-472.
807 Haltuch MA, Tolimieri N, Lee Q, Jacox MG. Oceanographic drivers of petrale sole recruitment
808 in the California Current Ecosystem, Fish. Ocean. 2020; 29:122-136. doi:
809 10.1111/fog.12459.
810 Hare SR, Mantua NJ. Empirical evidence for North Pacific regime shifts in 1977 and 1989. Prog.
811 Oceanogr. 2000; 47: 103–145. doi: 10.1016/s0079-6611(00)00033-1.
812 Harvey CJ, Fisher J, Samhouri, JF, Williams GD, Francis TB, Jacobson KC et al. The
813 importance of long-term ecological time series for integrated ecosystem assessment and
814 ecosystem-based management. Prog. Oceanogr. 2020. doi: 10.1016/j.pocean.2020.102418.
815 Hazen EL, Palacios DM, Forney KA, Howell EA, Becker E, Hoover AL et al. WhaleWatch: a
816 dynamic management tool for predicting blue whale density in the California Current. J.
817 Appl. Ecol. 2017. doi: 10.1111/1365-2664.12820.
818 Hazen EL, Scales KL, Maxwell SM, Briscoe D, Welch, H, Bograd et al. A dynamic ocean
819 management tool to reduce bycatch and support sustainable fisheries. Sci. Adv. 2018, 4:
820 eaar3001.
821 Hobday AJ, Oliver ECJ, Sen Gupta A, Benthuysen JA, Burrows MT, Donat MG et al.
822 Categorizing and naming marine heatwaves. Oceanography 2018; 31: 162 - 173.
823 Hobday AJ, Spillman CM, Paige Eveson J, Hartog JR. Seasonal forecasting for decision support
824 in marine fisheries and aquaculture. Fish. Oceanogr. 2016; 25: 45–56.
825 Hoffman MD, Gelman A. The No-U-Turn Sampler: Adaptively Setting Path Lengths in

826 Hamiltonian Monte Carlo. J. Mach. Learn. Res. 2014; 15: 1593–1623.
827 Holmes EE. Beyond theory to applications and evaluation: Diffusions approximations for
828 population viability analysis. Ecol. Appl. 2004; 14: 1272-1293.
829 Holmes EE, Ward EJ, Scheuerell, MD. Analysis of multivariate time series using the MARSS
830 package; 2018.
831 Jacox MG, Alexander MA, Siedlecki S, Chen K, Kwon Y-O, Brodie S et al. Seasonal-to-
832 interannual prediction of North American coastal marine ecosystems: Forecast methods,
833 mechanisms of predictability, and priority developments. Prog. Oceanogr. 2020. doi:
834 10.1016/j.pocean.2020.102307.
835 Jacox MG, Alexander MA, Stock CA, Hervieux G. On the skill of seasonal sea surface
836 temperature forecasts in the California Current System and its connection to ENSO
837 variability. Clim. Dyn. 2019; 53: 7519-7533.
838 Jacox MG, Alexander MA, Mantua NJ, Scott JD, Hervieux G. Webb RS et al. Forcing of
839 multiyear extreme ocean temperatures that impacted California Current living marine
840 resources in 2016. Bull. Am. Meteorol. Soc. 2018a; 99: S27–S33. doi: 10.1175/BAMS-D-
841 17-0119.1
842 Jacox MG, Edwards CA, Hazen EL, Bograd, SJ. Coastal upwelling revisited: Ekman, Bakun,
843 and improved upwelling indices for the U.S. west coast. J. Geophys. Res. 2018b.
844 doi:10.1029/2018JC014187.
845 Jones T, Parish JK, Peterson WT, Bjorkstedt EP, Bond NA, Balance LT et al. Massive mortality
846 of a planktivorous seabird in response to a marine heatwave. Geophys. Res. Lett. 2018; 45:
847 3193-3202.
848 Kaplan IC, Williams GD, Bond NA, Hernmann AJ, Siedlecki S. et al. Cloudy with a chance of

849 sardines: forecasting sardine distributions using regional climate models. Fish. Oceanogr.
850 2016; 25: 15-2.
851 Koslow J, Goericke R, Watson W. Fish assemblages in the Southern California Current:
852 relationships with climate, 1951–2008. Fish. Oceanogr. 2013; 22: 207–219.
853 Koslow JA, Hobday AJ, Boehlert GW et al. Climate variability and marine survival of coho
854 salmon (*Oncorhynchus kisutch*) in the Oregon production area. Fish. Oceanogr. 2002; 11: 65-
855 77.
856 Laufkötter C, Zscheischler J, Frölicher TL. High-impactmarine heatwaves attributable to human-
857 induced global warming. Science 2020; 369: 1621-1625.
858 Litzow MA, Ciannelli L. 2007. Oscillating trophic control induces community reorganization in
859 a marine ecosystem. Ecol. Lett. 2007; 10: 1124–1134. doi: 10. 1111/j.1461-
860 0248.2007.01111.x.
861 Litzow MA, Ciannelli L, Puerta P, Wettstein JJ, Rykaczewski RR, Opiekun M. Non-stationary
862 climate–salmon relationships in the Gulf of Alaska. Proc. R. Soc. B Biol. Sci. 2018; 285:
863 20181855. doi: 10.1098/rspb.2018.1855.
864 Litzow MA, Ciannelli L, Puerta P, Wettstein JJ, Rykaczewski RR, Opiekun M. Nonstationary
865 environmental and community relationships in the North Pacific Ocean. Ecology 2019; 100:
866 ecy.2760. doi: 10.1002/ecy.2760.
867 Litzow et al. 2020a. Evaluating ecosystem change as Gulf of Alaska temperature exceeds the
868 limits of preindustrial variability. Prog. Ocean. 2020a; 117: 7665-7671.
869 Litzow MA, Hunsicker ME, Bond NA, Burke BJ, Cunningham CJ, Gosselin JL, Norton EL,
870 Ward EJ, Zador SG. 2020b. The changing physical and ecological meanings of North Pacific
871 Ocean climate indices. Proc. Natl. Acad. Sci. U.S.A. 2020b; 117: 7665–7671. doi:

872 10.1073/pnas.1921266117.
873 Litzow MA, Malick MJ, Bond NA, Cunningham CJ, Gosselin JL, Ward EJ. 2020c. Quantifying
874 a novel climate through changes in PDO-climate and PDO-salmon relationships. Geophys.
875 Res. Lett. 2020b. doi: 10.1029/2020GL087972.
876 MacCall AD. Patterns of low-frequency variability in fish populations of the California Current.
877 CalCOFI Reports 1996; 37: 100-110.
878 Malick M.J, Siedlecki SA, Norton EL, Kaplan IC, Haltuch MA, Hunsicker ME et al. 2020.
879 Environmentally driven seasonal forecasts of Pacific hake distribution. Front. Mar. Sci. 7:
880 578490. doi: 10.3389/fmars.2020.578490.
881 Mantua NJ, Hare SR, Zhang Y, Wallace JM, Francis RC. A Pacific interdecadal climate
882 oscillation with impacts on salmon production. Bull. Am. Meteorol. Soc. 1997; 78, 1069–
883 1079.
884 McCabe RM, Hickey BM, Kudela RM, Lefebvre KA, Adams NG, Bill BD et al. An
885 unprecedented coastwide toxic algal bloom linked to anomalous ocean conditions. Geophys.
886 Res. Lett. 2016; 43: 10366–10376. doi:10.1002/2016GL070023.
887 McClatchie S, Goericke R, Koslow JA, Schwing FB, Bograd SJ, Charter R, W et al. The State of
888 the California Current, 2007–2008: La Niña conditions and their effects on the ecosystem.
889 Cal-COFI Rep. 2008; 49: 39–76.
890 McClatchie S, Goericke R, Schwing FB, Bograd SJ, Peterson WT, Emmett R et al. The state of
891 the California Current, 2008–2009: Cold conditions drive regional difference. CalCOFI
892 Rep. 2009; 50: 43–68
893 McClatchie S, Field J, Thompson AR, Gerrodette T, Lowry M, Fiedler PC et al. Food limitation
894 of sea lion pups and the decline of forage off central and southern California. R. Soc.

opensci. 2016; 3: 150628. doi: 10.1098/rsos.150628.

McGowan JA, Bograd SJ, Lynn RJ, Miller AJ. The biological response to the 1977 regime shift in the California Current. Deep Sea Res. II 2003; 50: 2567-2582.

Milly PCD, Betancourt J, Falkenmark M, Hirsch, RM, Kundzewicz ZW, Lettenmaier DP et al. On critiques of "Stationarity is dead: Whither water management?" Water Res. Res. 2015; 51: 7785–7789.

Möllmann C, Diekmann R. Marine Ecosystem Regime Shifts Induced by Climate and Overfishing: A Review for the Northern Hemisphere. Adv. Ecol. Res. 2012; 47: 303.347.

Morgan CA, Beckman BR, Weitkamp LA, Fresh KL. Recent ecosystem disturbance in the Northern California Current. Fisheries 2019; 44: 465-474. doi: 10.1002/fsh.10273.

Muhling B, Brodie S, Jacox MG, Snodgrass O, Dewar H, Tommasi D, Edwards C, Xu Y, Snyder S, Childers J. Dynamic habitat use of albacore and their primary prey species in the California Current System. CalCOFI Reports 2019; 60: 79-93.

Muhling B, Brodie S, Smith JA, Tommasi D, Gaitan CF, Hazen EL et al. Predictability of species distributions deteriorates under novel environmental conditions in the California Current System. Front. Mar. Sci. 2020; doi:10.3389/fmars.2020.00589.

Neveu E, Moore AM, Edwards CA, Fiechter J, Drake P, Jacox MG, Nuss E. A historical analysis of the California Current using ROMS 4D-Var. Part I: System configuration and diagnostics, Ocean Model. 2016; 99: 133-151. doi:10.1016/j.ocemod.2015.11.012.

Nielsen JM, Rogers LA, Brodeur RD, Thompson AR, Auth TD, Dreary AL et al. Responses of ichthyoplankton assemblages to the recent marine heatwave and previous climate fluctuations in several Northeast Pacific marine ecosystems. Glob. Chang. Biol. 2020; 27: 506-520.

Nieto K, McClatchie S, Weber ED, Lennert-Cody CE. Effect of mesoscale eddies and streamers on sardine spawning habitat and recruitment success off Southern and central California, J. Geophys. Res. Oceans 2014; 119: 6330–6339, doi:10.1002/014JC010251.

Peabody CE, Thompson AR, Sax DF, Morse RE, Perretti CT. Decadal regime shifts in southern California's ichthyoplankton assemblage. Mar. Ecol. Prog. Ser. 2018; 607: 71-83.

Peterson WT, Emmett R, Goericke R, Venrick E, Mantyla A, Bograd S et al. The State of the California Current, 2005-2006: warm in the north, cool in the south. CalCOFI Reports 2006; 47: 30–74.

Peterson et al. 2015 https://agupubs.onlinelibrary.wiley.com/doi/full/10.1002/2017JC012952

Piatt JF, Parrish JK, Renner HM, Schoen SK, Jones TT, Arimitsu ML et al. Extreme mortality and reproductive failure of common murres resulting from the northeast Pacific marine heatwave of 2014-2016. PLoSONE 2020; 15: e0226087. doi: 10.1371/journal.pone.0226087

Planque B, Arneberg P. 2018. Principal component analyses for integrated ecosystem assessments may primarily reflect methodological artefacts. ICES J. Mar. Sci. 2018; 75: 1021–1028.

Puerta P, Ciannelli L, Rykaczewski R, Opiekun M, Litzow MA. Do Gulf of Alaska fish and crustacean populations show synchronous non-stationary responses to climate? Prog. Oceanogr. 2019; 175: 161–170. doi: 10.1016/j.pocean.2019. 04.002.

R Core Team. R: A language and environment for statistical computing. R Foundation for Statistical Computing, Vienna, Austria, 2021.

Ralston S, Sakuma KM, Field JC. Interannual variation in pelagic juvenile

941 rockfish (Sebastes spp.) abundance – going with the flow. Fish. Ocean. 2013; 22:288–308.
942 doi: 10.1111/fog.12022.
943 Ralston S, Field JC, Sakuma KM. Long-term variation in a central Californiapelagic forage
944 assemblage. J. Mar. Sys. 2015; 146: 26-37. doi: 10.1016/j.jmarsys.2014.06.013.
945 Ryan JP, Kudela RM, Birch JM, Blum M, Bowers HA, Chavez FP et al. Causality of an extreme
946 harmful algal bloom in Monterey Bay, California, during the 2014–2016 northeast Pacific
947 warm anomaly. Geophys. Res. Lett. 2017; 44: 5571-5579. doi: 10.1002/2017GL072637.
948 Sakuma KM, Field JC, Mantua NJ, Ralston S, Marinovic BB, Carrion CN.
949 Anomalous epipelagic micronekton assemblage patterns in the neritic waters of the
950 California Current in spring 2015 during a period of extreme ocean conditions. CalCOFI
951 Reports 2016; 57: 163-183.
952 Sanford E, Sones JL, García-Reyes M, Goddard JH, Largier JL. Widespread shifts in the coastal
953 biota of northern California during the 2014–2016 marine heatwaves. Sci. Rep. 2019; 9: 1-
954 14.
955 Santora JA, Mantua NJ, Schroeder ID, Field JC, Hazen E, Bograd SJ et al. Habitat compression
956 and ecosystem shifts as potential links between marine heatwave and record whale
957 entanglements. Nat. Commun. 2020; 11: 1-12.
958 Santora JA, Hazen EL, Schroeder ID, Bograd SJ, Sakuma KM, Field JC. Impacts of ocean
959 climate variability on biodiversity of pelagic forage species in an upwelling ecosystem.
960 Mar. Ecol. Prog. Ser. 2017; 580: 205-220.
961 Santora JA, Schroeder ID, Field JC, Wells BK, Sydeman WJ. 2014. Spatiotemporal
962 dynamics of ocean conditions and forage taxa reveals regional structuring of predator-prey
963 relationships. Ecol. Appl. 2014; 24:1730-1747. doi:10.1890/13-1605.1.

964 Schroeder ID, Santora JA, Bograd SJ, Hazen EL, Sakuma, KM, Moore AM et al. Source water
965 variability as a driver of rockfish recruitment in the California Current Ecosystem:
966 implications for climate change and fisheries management. Can. J. Fish. Aquat. Sci. 2019;
967 76: 950-960. doi: 10.1139/cjfas-2017-0480.
968 Schwartzlose RA, Alheit J, Bakun A, Baumgartner TR, Cloete R, Crawford RJM et al. 1999.
969 Worldwide large-scale fluctuations of sardine and anchovy populations. S. Afr. J. Mar. Sys.
970 1999; 21: 289-347.
971 Sen Gupta A, Thomsen M, Benthuysen JA. *et al.* Drivers and impacts of the most extreme
972 marine heatwaves events. Sci. Rep. 2020; 10: 19359. doi: 10.1038/s41598-020-75445-3.
973 Seo H, Brink KH, Dorman E, Koracin D, Edwards CA. What determines the spatial pattern in
974 summer upwelling trends on the US West Coast? J. Geophys. Res. Oceans 2012. doi:
975 10.1029/2012JC008016.
976 Siedlecki SA, Kaplan IC, Hermann AJ, Nguyen TT, Bond NA, Newton JA et al. Experiments
977 with seasonal forecasts of ocean conditions for the northern region of the California
978 Current upwelling system. Sci. Rep. 2016; 6: 27203. DOI: 10.1038/srep27203.
979 Siegelman-Charbit L, Koslow JA, Jacox MG, Hazen EL, Bograd SJ, Miller EF, McGowan JA.
980 Physical forcing on fish abundance in the southern California Current System. Fish. Ocean.
981 2018; 27: 475–488. doi:10.1111/fog.12267.
982 Stan Development Team. RStan: The R interface to Stan. 2018.
983 Sydeman WJ, Dedman S, Garcia-Reyes M, Thompson SA, Thayer JA, Bakun A, MacCall AD.
984 Sixty-five years of northern anchovy population studies in the southern California Current: a
985 review and suggestion for sensible management. ICES J. Mar. Sci. 2020; 77: 486–499.

Thompson AR, Hyde JR, Watson W, Chen DC, Guo LW. Rockfish assemblage structure and spawning locations in southern California identified through larval sampling. Mar. Ecol. Prog. Ser. 2016; 547: 177-192.

Thompson AR, Schroeder ID, Bograd SJ, Hazen EL, Jacox MG, Leising AL et al. State of the California Current 2018-19: a novel anchovy regime and a new marine heatwave? CalCOFI Reports 2019; 60: 1-65.

Tolimieri N, Haltuch M, Lee Q, Jacox MG, Bograd SJ. Oceanographic drivers of sablefish recruitment in the California Current. Fish. Ocean, 2018; 27: 458-474, doi:10.1111/fog.12266.

Tommasi D, Stock CA, Hobday AJ, Methot R, Kaplan IC, Eveson JP et al. Managing living marine resources in a dynamic environment: the role of seasonal to decadal climate forecasts. Prog. Oceanogr. 2017; 152: 15–49.

Vehtari A, Gelman A, Gabry J. Practical Bayesian model evaluation using leave-one-out cross-validation and WAIC. Statistics and Computing 2017; 27: 1413-1432. doi: 10.1007/s11222-016-9696-4.

Walker Jr HJ, Hastings PA, Hyde JR, Lea RN, Snodgrass OE, Bellquist LF. Unusual occurrences of fishes in the Southern California Current System during the warm water period of 2014–2018. Estuar. Coast. Shelf Sci. 2020; 236: 106634.

Walsh JE, Thoman RL, Bhatt US, Bieniek PA, Brettschneider B, Brubaker M et al. The high latitude heat wave of 2016 and its impacts on Alaska. Bull. Am. Meteorol. Soc. 2018; 99: S39–S43. doi: 10.1175/BAMS-D-17-0105.

Ward EJ, Holmes EE, Thorson JT, Collen B. Complexity is costly: a meta-analysis of parametric and non-parametric methods for short-term population forecasting. Oikos 2014; 123: 652-

661.

Ward EJ, Anderson SC, Damiano LA, Hunsicker ME, Litzow MA. Modeling regimes with extremes: the bayesdfa package for identifying and forecasting common trends and anomalies in multivariate time-series data. R J 2019; 11: 46–55.

Ward EJ, Anderson SC, Damiano LA, Malick MJ. bayesdfa: Bayesian Dynamic Factor Analysis (DFA) with 'Stan'. R package version 1.1.0 2020. https://CRAN.R-project.org/package=bayesdfa

Welch H, Hazen EL, Briscoe DK, Bograd SJ, Jacox MG, Eguchi T et al. Environmental indicators to reduce loggerhead turtle bycatch offshore of Southern California. Ecol. Ind. 2019; 98: 657-664. doi:10.1016/j.ecolind.2018.11.001.

Wells BK, Field JC, Thayer JA, Grimes CB, Bograd SJ, Sydeman WJ et al. Untangling the relationships among climate, prey and top predators in an ocean ecosystem. Mar. Ecol. Prog. Ser. 2008; 364: 15-29.

Wernberg T, Bennett S, Babcock RC, De Bettignies T, Cure K, Depczynksi M et al. Climate-driven regime shift of a temperate marine ecosystem. Science 2016; 353: 169-172.

Zuur AF, Tuck ID, Bailey N. Dynamic factor analysis to estimate common trends in fisheries time series. Can. J. Fish. Aquat. Sci. 2003; 60: 542–552.

Supporting Information

S1 Appendix: Standardization of time series from spatially resolved datasets.

S1 Table: Climate and biology time series included in the analyses

S2 Table: Summary information for the Bayesian DFA biology-covariate and biology only models (years 1981–2017).

S3 Table: Observations, predictions, and prediction errors for single species parameters in 2018.

S1 Figure: Climate and biology time series used in the study analyses.

S2 Figure: AR(1) coefficient on the southern/central California latent climate trend and support for a heavy-tailed deviations of the latent trend.

S3 Figure: The Student-t deviations degrees of freedom parameter (nu) in the southern/central California biology trend.

S4 Figure: A summary of the effect of the Cumulative Upwelling Transport Index (CUTI) on the individual single species parameter included in the DFA analyses

S5 Figure: A summary of the effect of the Isothermal Layer Depth (ILD) on the individual single species parameter included in the DFA analyses.

S6 Figure: A summary of the effect of the sea surface temperature on the individual single species parameter included in the DFA analyses

S7 Figure: Community variability in the southern California Current ecosystem (1981–2018).

S8 Figure: Forecasts and model estimates of the 'true' community state in the southern and central California Current in years 2009–2018.

S9 Figure: Fitted values for biology-covariate model including BEUTI (nitrate flux) as a covariate (1981–2017).

S10 Figure: Log coefficient of variation (CV) of 2018 predictions of individual species parameters plotted against the mean and log CV of loadings related to each species, and the mean and log CV of coefficients relating each species to BEUTI (nitrate flux).

Figure 1

Click here to access/download;Figure;Figure_1_CCE study area.jpeg

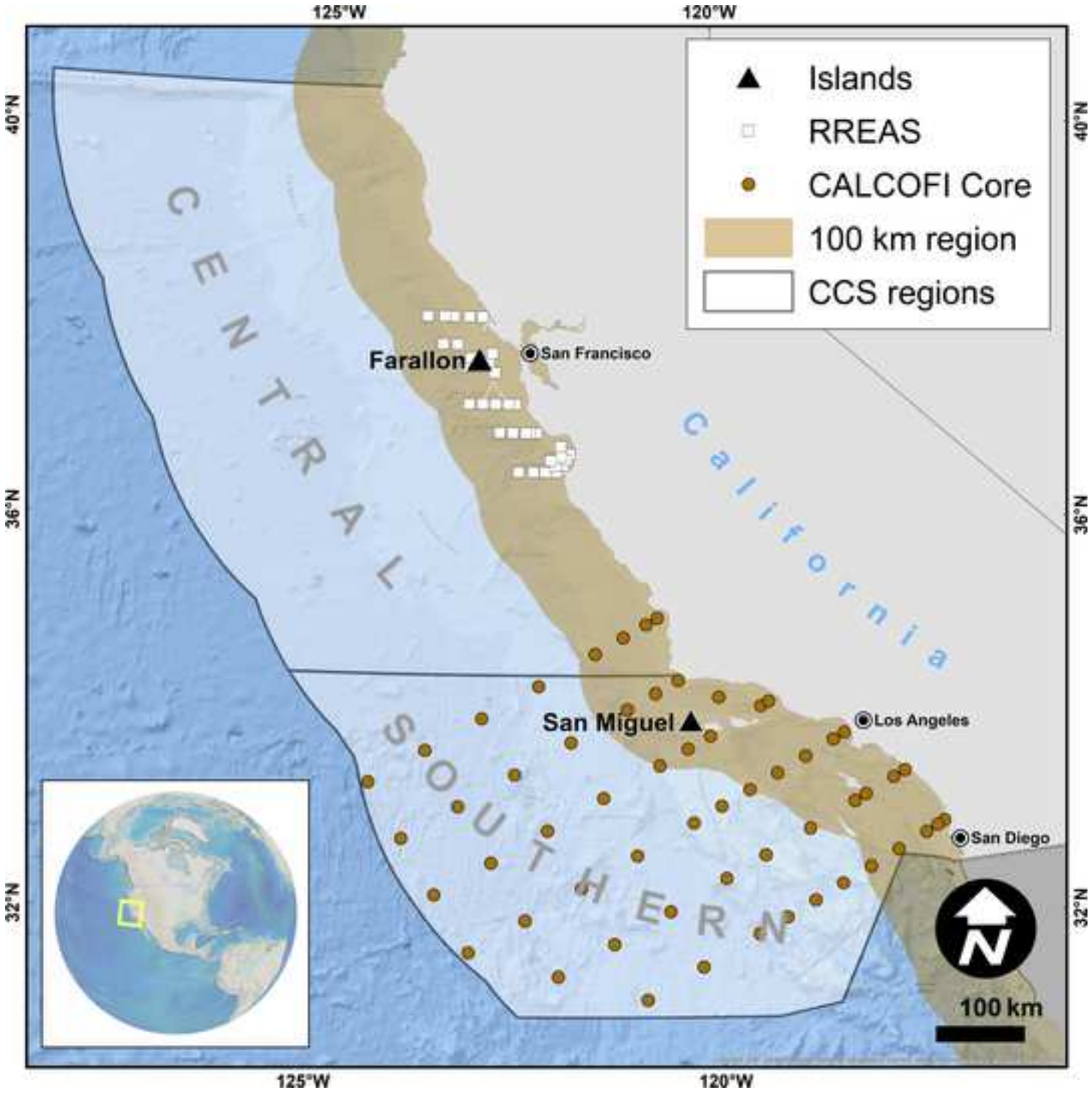

Figure 2a

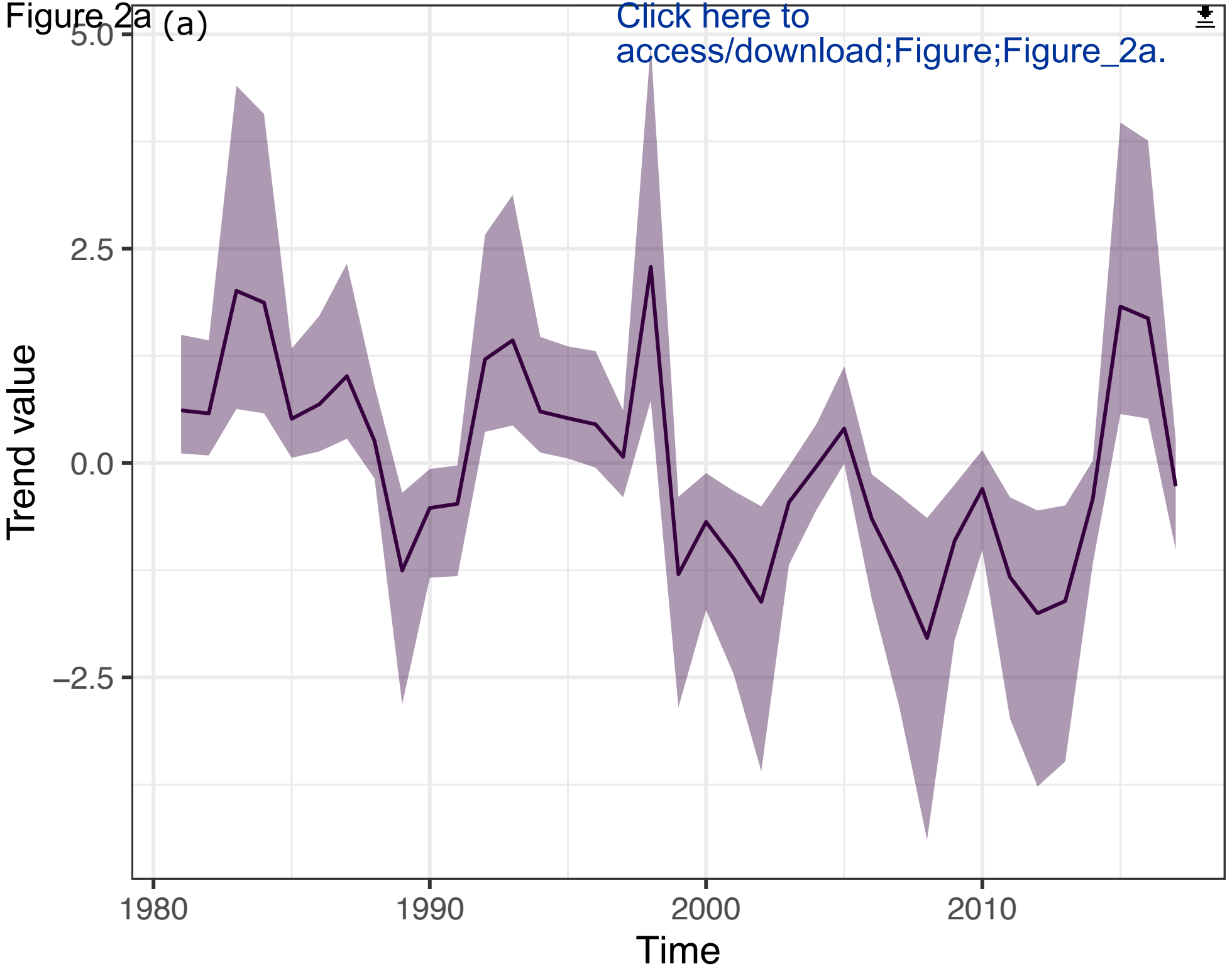
(a)
Click here to access/download;Figure;Figure_2a.
5.0
2.5
0.0
−2.5
Trend value
1980
1990
2000
2010
Time

Figure 2b

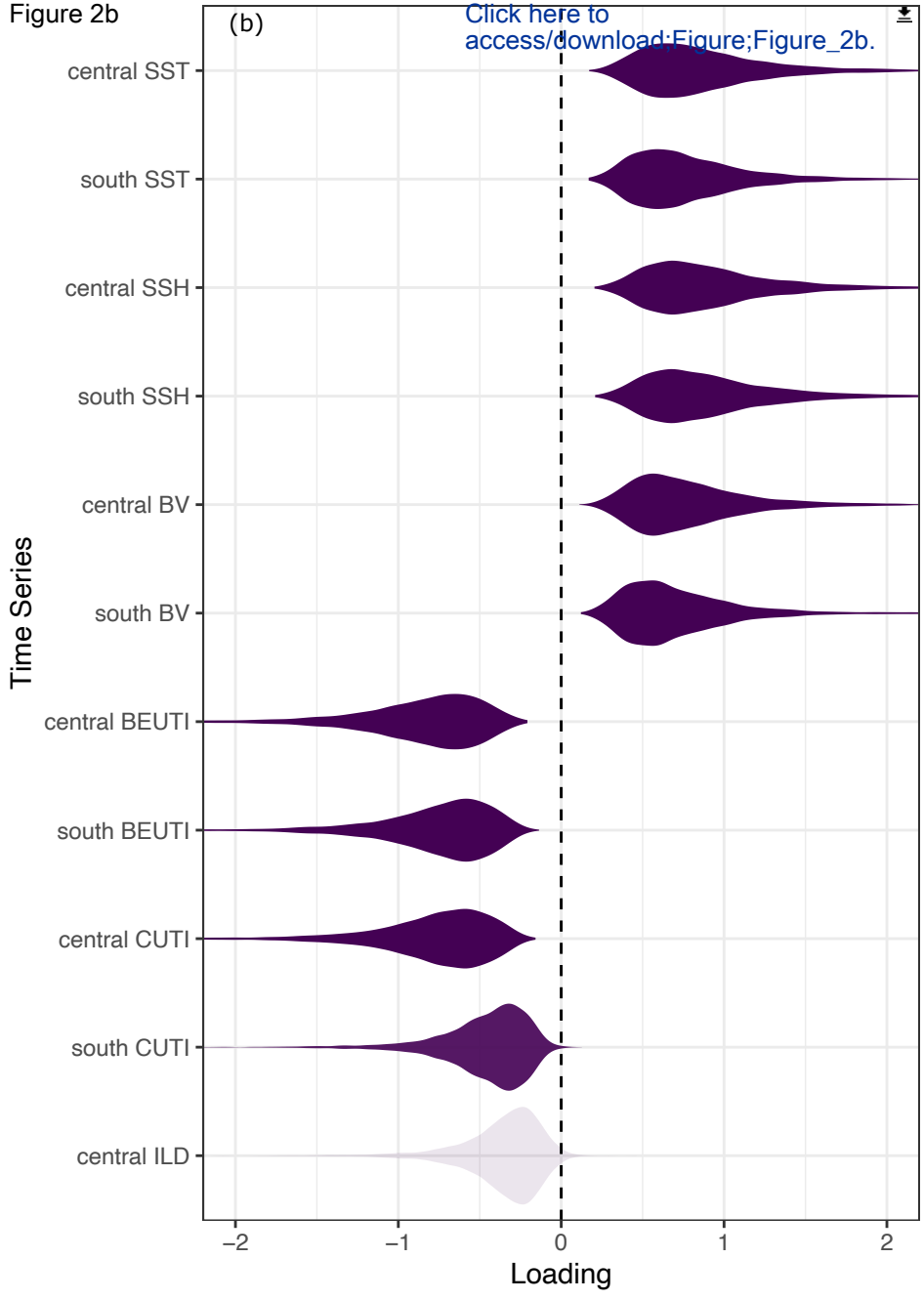
(b)
Click here to access/download;Figure;Figure_2b.
central SST
south SST
central SSH
south SSH
central BV
south BV
central BEUTI
south BEUTI
central CUTI
south CUTI
central ILD
Time Series
−2
−1
0
1
2
Loading

Figure 3a Climate

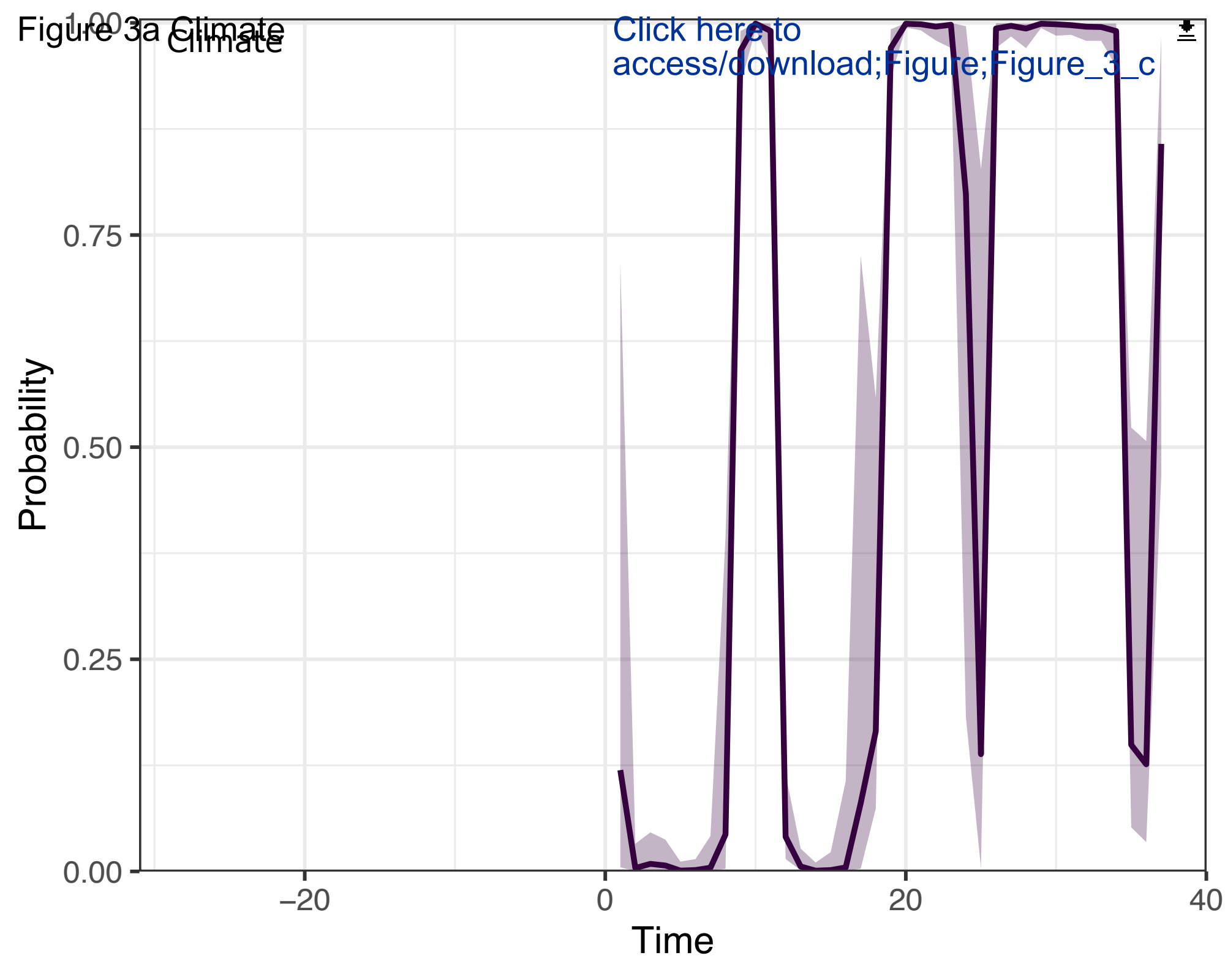

Figure 3b Biology

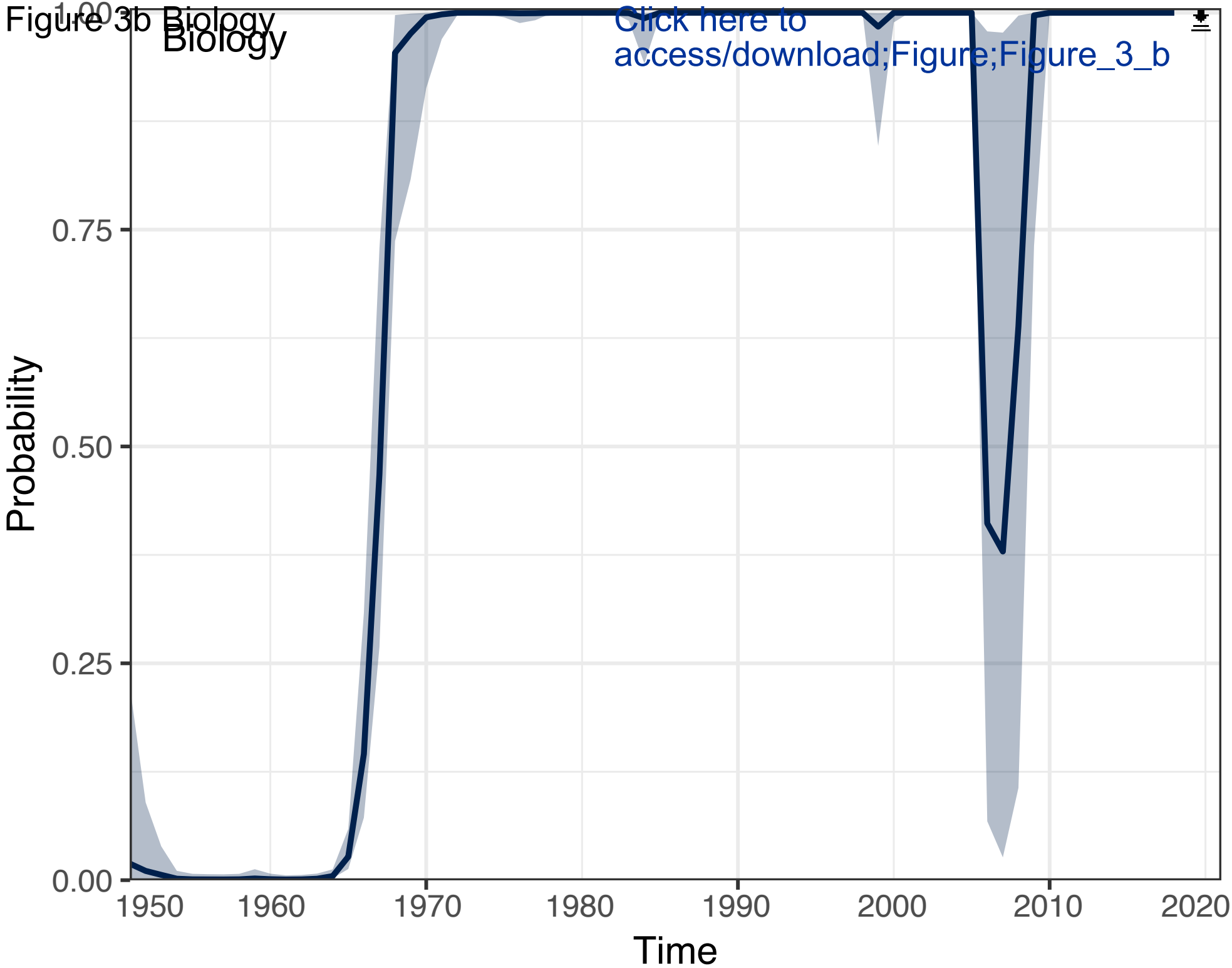

Figure 4a

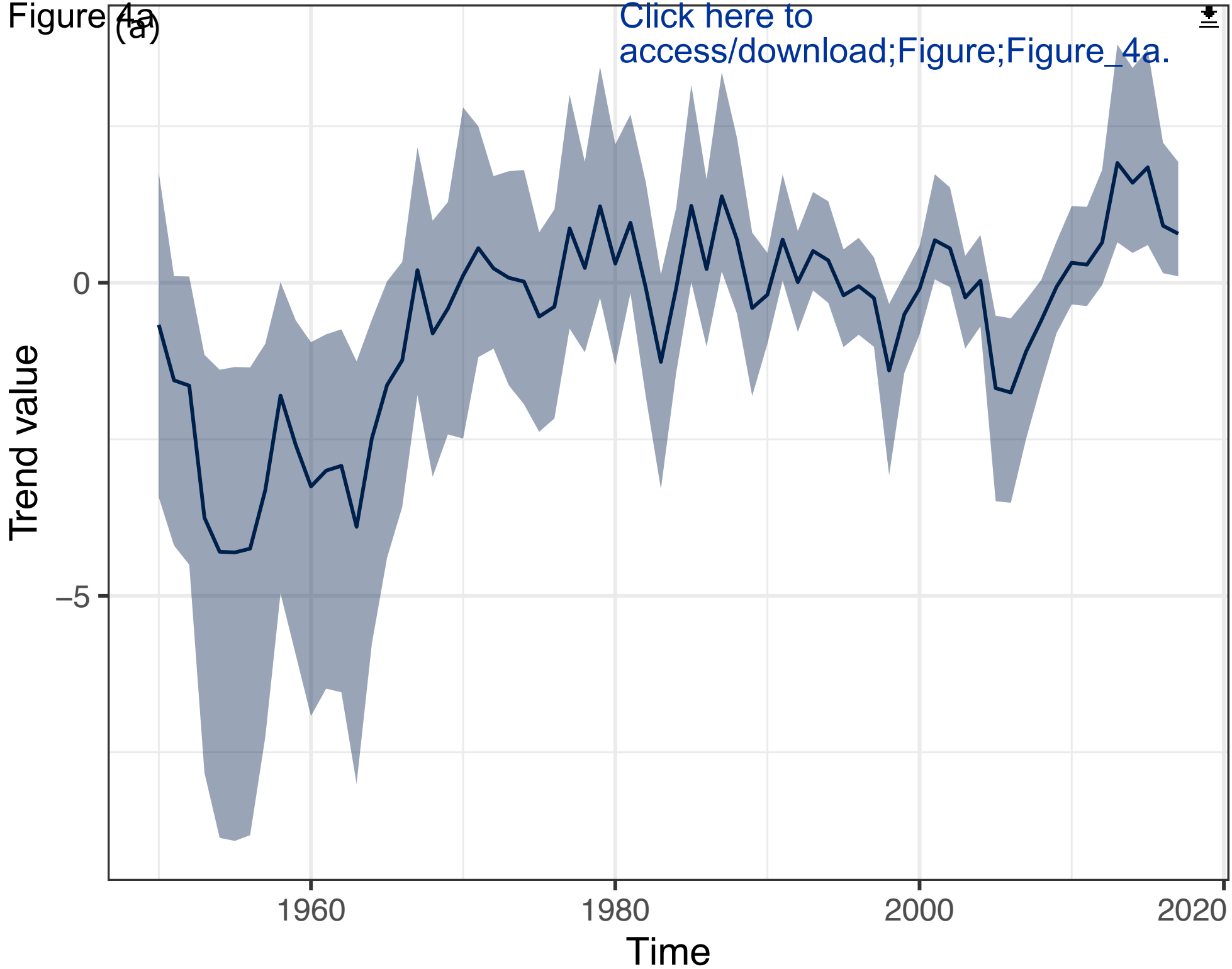
(a)
Click here to access/download;Figure;Figure_4a.
Trend value
0
−5
1960
1980
2000
2020
Time

Figure 4b

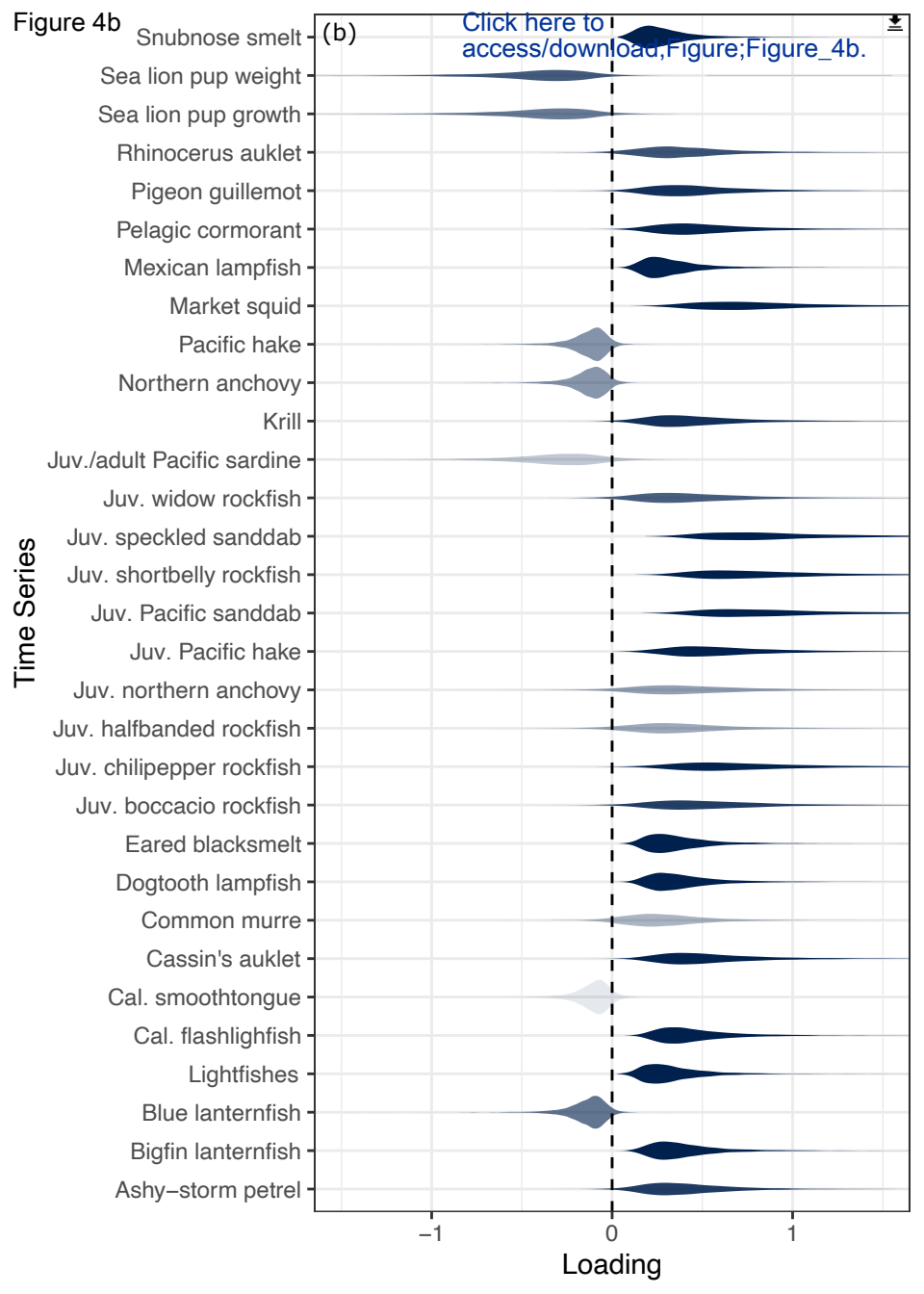
(b)
Click here to access/download;Figure;Figure_4b.
Snubnose smelt
Sea lion pup weight
Sea lion pup growth
Rhinocerus auklet
Pigeon guillemot
Pelagic cormorant
Mexican lampfish
Market squid
Pacific hake
Northern anchovy
Krill
Juv./adult Pacific sardine
Juv. widow rockfish
Juv. speckled sanddab
Juv. shortbelly rockfish
Juv. Pacific sanddab
Juv. Pacific hake
Juv. northern anchovy
Juv. halfbanded rockfish
Juv. chilipepper rockfish
Juv. boccacio rockfish
Eared blacksmelt
Dogtooth lampfish
Common murre
Cassin's auklet
Cal. smoothtongue
Cal. flashlighfish
Lightfishes
Blue lanternfish
Bigfin lanternfish
Ashy–storm petrel
Time Series
−1
0
1
Loading

Figure 5

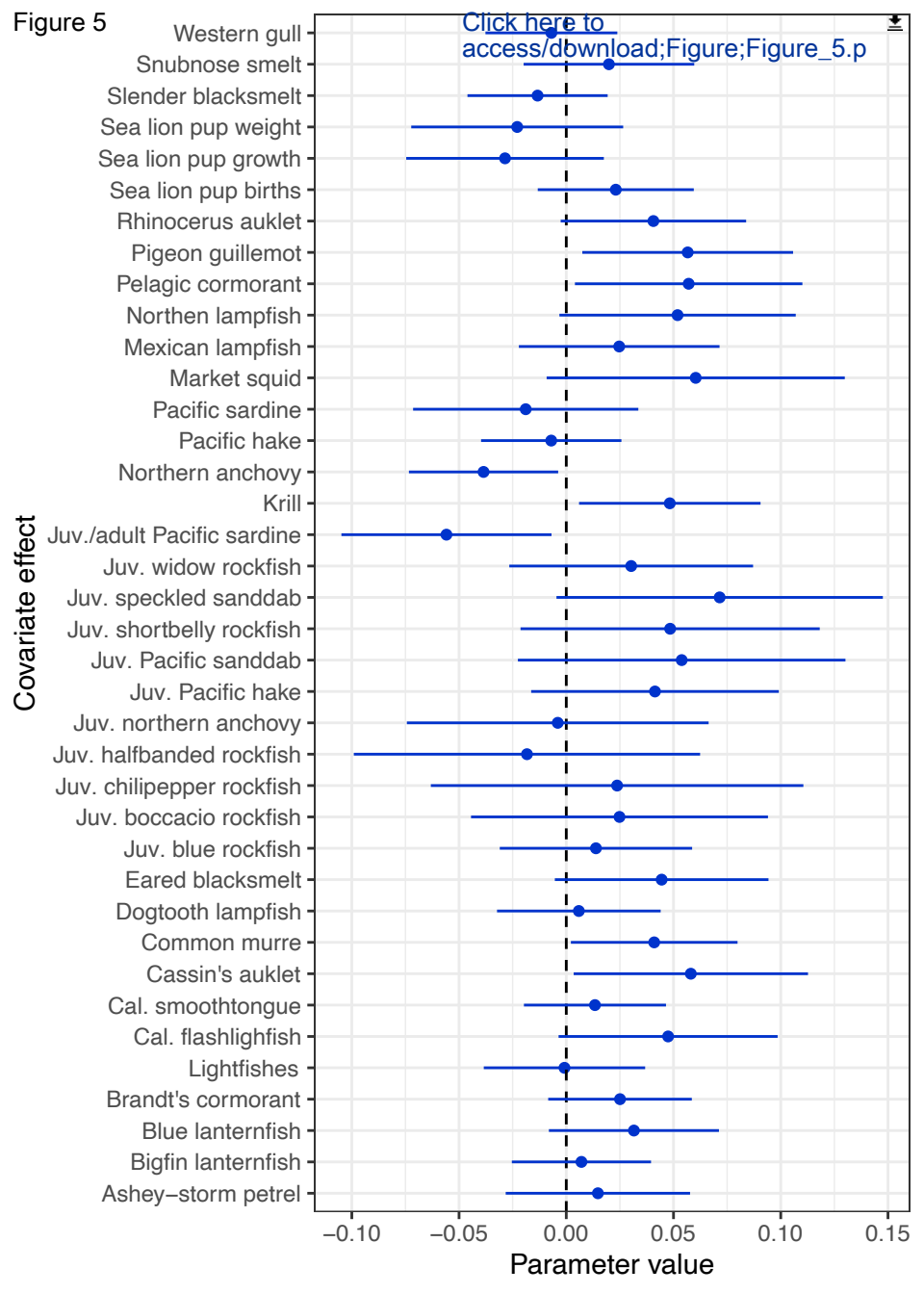
Click here to access/download;Figure;Figure_5.p
Western gull
Snubnose smelt
Slender blacksmelt
Sea lion pup weight
Sea lion pup growth
Sea lion pup births
Rhinocerus auklet
Pigeon guillemot
Pelagic cormorant
Northen lampfish
Mexican lampfish
Market squid
Pacific sardine
Pacific hake
Northern anchovy
Krill
Juv./adult Pacific sardine
Juv. widow rockfish
Juv. speckled sanddab
Juv. shortbelly rockfish
Juv. Pacific sanddab
Juv. Pacific hake
Juv. northern anchovy
Juv. halfbanded rockfish
Juv. chilipepper rockfish
Juv. boccacio rockfish
Juv. blue rockfish
Eared blacksmelt
Dogtooth lampfish
Common murre
Cassin's auklet
Cal. smoothtongue
Cal. flashlighfish
Lightfishes
Brandt's cormorant
Blue lanternfish
Bigfin lanternfish
Ashey–storm petrel
Covariate effect
−0.10
−0.05
0.00
0.05
0.10
0.15
Parameter value

Figure 6

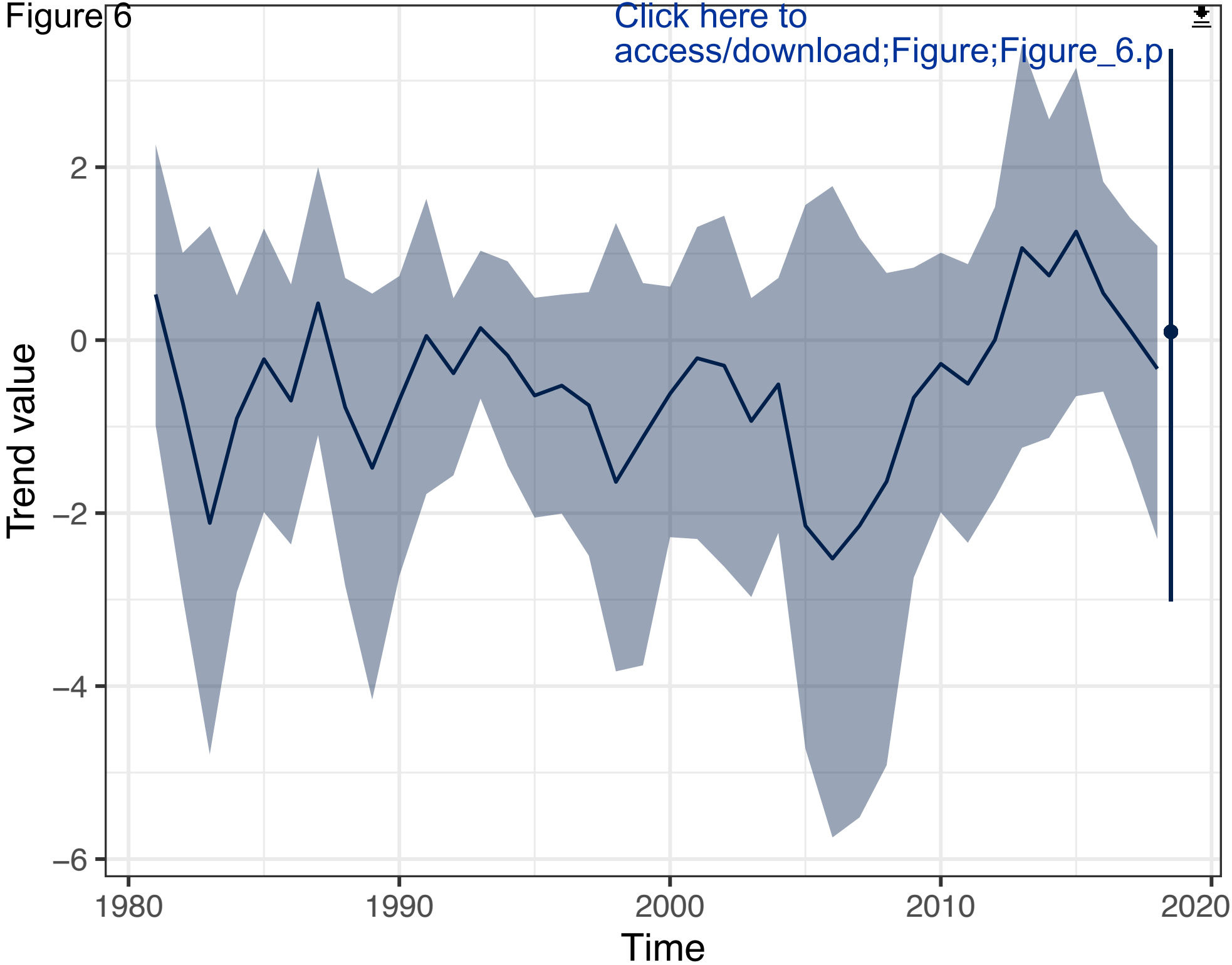
Click here to
access/download;Figure;Figure_6.p
Trend value
2
0
−2
−4
−6
1980
1990
2000
2010
2020
Time